Supporting information for:

Synthesis, Photophysical and Concentration Dependent Tunable Lasing Behaviour of 2,6-Diacetynyl Functionalized BODIPY Dyes

Apurba Maity,[a] Anirban Sarkar,[b]Amit Sil,[a] Shivakiran Bhaktha B. N,[*b] Sanjib K. Patra[*a]

[a]*Department of Chemistry, Indian Institute of Technology Kharagpur, Kharagpur 721302, INDIA*

[b]*Department of Physics, Indian Institute of Technology Kharagpur, Kharagpur 721302, INDIA*

Contents

1. Synthetic and Characterization

1.a) Synthesis

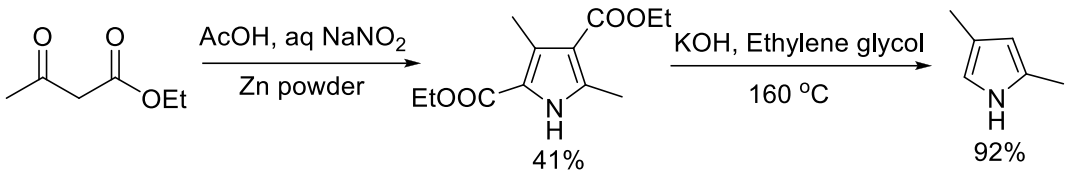

Diethyl 3,5-dimethyl-1H-pyrrole-2,4-dicarboxylate[1]: An aqueous solution of sodium nitrite (5.4 g, 78.4 mmol) in water (10 mL) was added to a mixture of ethyl acetoacetic ester (20.4 gm, 20 mL, 156.8 mmol) and acetic acid (40 mL) over 30 min under ice cool condition to keep the temperature below 10 ˚C. The yellowish clear solution was formed which was allowed to stir for another 2.5 h at 10˚C to complete the reaction. Then zinc powder (9.60 g, 156.8 mmol) was added to this mixture portion wise while the reaction mixture was kept below 25˚C. Next the reaction mixture was heated to 45–50˚C for 10 min and then continued to 95 ˚C for another 1 h. After cooling down to room temperature yellowish precipitate was formed which was filtered off and washed with ice water (100 mL) to remove the AcOH. The yellow crude solid was recrystallized from ethanol to afford a pale yellow crystalline powder of pure compound **1** (15.4 gm, 41%). ^{1}H NMR (400 MHz $CDCl_3$) δ: (ppm): 8.90 (br s, 1H, pyrrole N-H), 4.35-4.26 (m, 4H, ester O-CH_2), 2,56 (s, 3H, pyrrole-CH_3), 2.51 (s, 3H, pyrrole-CH_3), 1.38-1.34(m, 6H, ester CH_3).

2,4-Dimethyl-1H-pyrrole[2]: In a 250ml schlenk flask purged with argon, compound **1** (2.0g, 8.35 mmol), KOH (2.34g, 41.8 mmol) were charged and heated to reflux in ethylene glycol (15 mL) for 4 hours at 160 ˚C. After cooling to room temperature, the reaction mixture was extracted with $CHCl_3$, washed with brine solution and dried over Na_2SO_4. The solvent was removed by rotary evaporation to furnish compound 2 as dark brown oil (0.73 gm, 92%) which was used without further purification. ^{1}H NMR (400 MHz $CDCl_3$) δ(ppm): 7.62 (br s, 1H, pyrrole N-H), 6.41(s, 1H, pyrrole H), 5.75(s, 1H, pyrrole H), 2.24 (s, 3H, pyrrole-CH_3), 2.08 (s, 3H, pyrrole-CH_3).

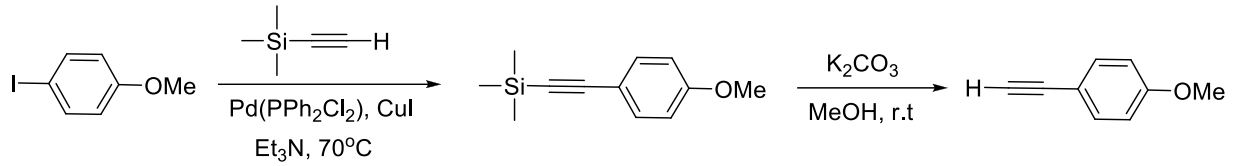

[(4-methoxyphenyl)ethynyl]trimethylsilane[3]: To a 100 mL Schlenk flask purged with argon, a mixture of 4-iodoanisole (0.5 g, 2.14 mmol), trimethylsilylacetylene (0.32 mL, 2.35 mmol), $Pd(PPh_3)_2Cl_2$ (0.045 g, 0.064 mmol) and CuI (0.025 g, 0.13 mmol) was added to a mixed solvent of Et_3N (2mL) and DMF (4mL). The reaction mixture was allowed to stir and heat at 50 °C for 8 h. Then the mixture was brought to ambient temperature and H_2O was added. The aqueous layer was separated and extracted with Et_2O. The combined organic layer was washed several times with H_2O, dried over Na_2SO_4, filtered and concentrated under reduced pressure. The residue was purified by column chromatography on silica gel (60-120 mesh) using 2% EtOAc in hexane as eluent to afford (4-Iodophenylethynyl)trimethylsilane (0.41 g, 94%) as a yellow oil. ^{1}H NMR (400 MHz $CDCl_3$) δ: (ppm): 7.40 (d, 8Hz, 2H, aryl-H), 6.81 (d, 8Hz, 2H, aryl-H), 3.80 (s, 3H, -OCH_3), 0.23 (s, 9H, TMS-CH_3). ^{13}C {^{1}H} NMR (100 MHz, $CDCl_3$): 159.9, 133.7, 115.5, 114.0, 105.4, 92.6, 55.5, 0.28

4-Ethynylanisole[4]: (4-Iodophenylethynyl)trimethylsilane (0.4 g, 1.94 mmol) was dissolved in 5 mL of methanol. Then K_2CO_3 (0.4 g, 2.91 mmol) was added to it and allowed to stir at room temperature for 3 h. Once the reaction is over, H_2O was added, extracted with EtOAc, dried over Na_2SO_4, evaporated under low pressure and purified through flash column chromatography using hexane as eluent to furnish 4-ethynylanisole (0.2 g, 78%) as pale yellow oil. ^{1}H NMR (400 MHz $CDCl_3$) δ: (ppm): 7.41 (d, 8Hz, 2H, aryl-H), 6.84 (d, 8Hz, 2H, aryl-H), 3.81 (s, 3H, -OCH_3), 3.00 (s, 1H, alkynyl-H). ^{13}C {^{1}H} NMR (100 MHz, $CDCl_3$): 160.1, 133.7, 114.1, 114.3, 83.8, 75.9, 55.4

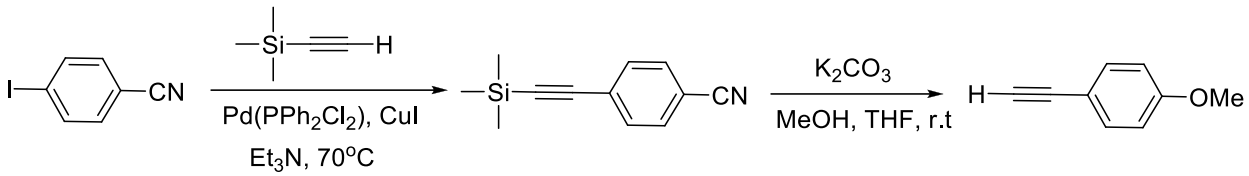

4-[(Trimethylsilyl)ethynyl]benzonitrile[5]: An oven dried 500 mL Schlenk flask was charged with 4-iodobenzonitrile (0.8 g, 3.5 mmol), Pd $(PPh_3)_2Cl_2$ (122 mg, 0.17 mmol), CuI (67 mg, 0.35 mmol) under argon atmosphere, then dry THF (6 mL), and dry triethylamine (10 mL) were added. Next trimethylsilylacetylene (0.52 g, 0.74 mL, 5.25 mmol) was added, and the reaction mixture was stirred at room temperature for 14 h. After completion of the reaction monitored by TLC analysis, the reaction mixture was diluted with diethyl ether (50 mL), and the precipitate was filtered through a pad of celite, and the filtrate was concentrated under reduced pressure. The residue was purified by column chromatography on silica gel (60-120 silica gel, 5% EtOAc in hexane as eluent) to afford the title compound (0.61 g) as a pale yellow solid in 87% yield. ^{1}H NMR (400 MHz $CDCl_3$) δ: (ppm): 7.59 (d, 8Hz, 2H, aryl-H), 7.53 (d, 8Hz, 2H, aryl-H), 0.26 (s, 9H, TMS-CH_3). ^{13}C {^{1}H} NMR (100 MHz, $CDCl_3$): 132.6, 132.1, 128.2, 118.6, 111.9, 103.2, 99.7, 0.10.

4-Ethynylbenzonitrile[5]: In a 100 mL Schlenk flask, 4-[(Trimethylsilyl)ethynyl]benzonitrile (0.3 g, 1.5 mmol) was dissolved in the mixture of THF (5 mL) and methanol (5 mL). Then Potassium carbonate (2 g, 15 mmol) was added, and suspension was vigorously stirred at room temperature for 12 h. The crude product was diluted with diethyl ether (50 mL), and passed through a short pad of silica gel. After evaporation, and drying under vacuo at room temperature, the title compound was obtained as white solid (0.18 g, 96% yield). ^{1}H NMR (400 MHz $CDCl_3$) δ: (ppm): 7.62 (d, 8Hz, 2H, aryl-H), 7.57 (d, 8Hz, 2H, aryl-H), 3.30 (s, 1H, alkynyl-H). ^{13}C {^{1}H} NMR (100 MHz, $CDCl_3$): 132.8, 132.2, 127.2, 118.4, 112.5, 82.0, 81.8.

Synthesis of 1. In an oven dried 250mL Schlenk flask, acetyl chloride (0.22 mL, 0.25 g, 3.15 mmol) was added dropwise to a solution of 2,4-dimethylpyrrole (0.65 mL, 0.6 g, 6.3 mmol) in anhydrous CH_2Cl_2 (100 mL) via syringe under argon atmosphere and the mixture was stirred at room temperature overnight. Then Et_3N (6 mL, 43 mmol) followed by BF_3•Et_2O (6 mL, 45-50% BF_3 in ether) were added under ice-cold condition, and the reaction mixture was stirred for additional 1 h. After that, the reaction mixture was poured into distilled water (100 mL). Organic

layer was extracted with dichloromethane (DCM), dried over anhydrous Na_2SO_4 and the solvent was evaporated under reduced pressure. The crude product was further purified using column chromatography (silica gel 60-120, CH_2Cl_2: hexane = 1:1) to give compound **1** as red powder. Yield: 0.35 g (42%). ^{1}H NMR (400 MHz, $CDCl_3$): 6.05 (s, 2H, pyrrole-H), 2.58 (s, 3H, meso-CH_3), 2.52 (s, 6H, pyrrole-CH_3), 2.41 (s, 6H, pyrrole-CH_3). ^{13}C{H} NMR ($CDCl_3$, 100 MHz): δ 153.8, 141.6, 141.2, 132.3, 121.5 (BODIPY core), 17.5, 16.9, 14.6 (-CH_3). ^{19}F{H} NMR (376 MHz, $CDCl_3$): δ -146.7 (q, J_{BF} = 34.0 Hz). HRMS (ESI$^+$, m/z): $[M+H]^+$ calcd for $C_{14}H_{18}BF_2N_2$ 263.1531, found 263.1547.

Synthesis of 2. In a 250 mL of Schlenk flask, NIS (1.35 g, 6 mmol) was charged to a solution of 1 (0.39 g, 1.5 mmol) in 70 mL of DCM under argon atmosphere. The reaction flask was covered with aluminium foil to protect it from light. The mixture was stirred for 12 h at room temperature (28 °C). After that the reaction mixture was washed with saturated aqueous $Na_2S_2O_3$ solution (3×30 mL) and dried over anhydrous Na_2SO_4. Volatiles were removed in vacuo. The crude material was purified over silica gel column chromatography using DCM as the eluent to get the title compound as an orange solid (0.65 gm, 85%). ^{1}H NMR ($CDCl_3$, 400 MHz): δ = 2.63 (s, 3H, meso-CH_3), 2.61 (s, 6H, pyrrole –CH_3), 2.47 (s, 6H, pyrrole –CH_3). ^{13}C{H} NMR ($CDCl_3$, 100 MHz): δ 155.3, 143.1, 141.3, 132.4, 86.0 (BODIPY core), 20.0, 18.1, 16.2 (-CH_3). ^{19}F{H} NMR (376 MHz, $CDCl_3$): δ -145.8 (q, J_{BF} = 34 Hz). MALDI-TOF MS: (m/z) calcd for $C_{14}H_{16}BF_2I_2N_2$ $[M+H]^+$, 514.946; found, 514.431.

1.b. NMR Spectra

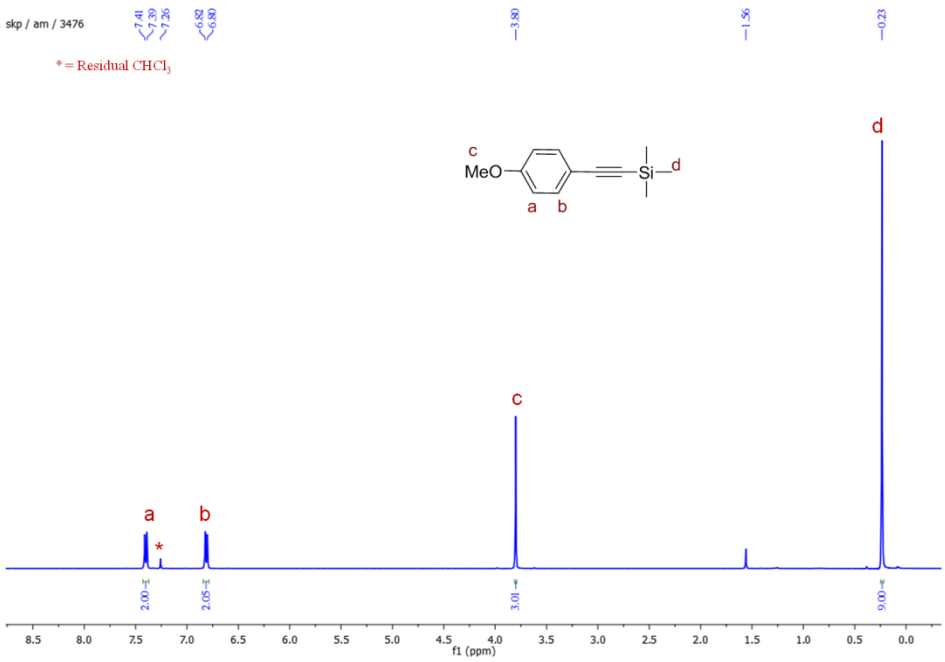

Fig S1: ^{1}H NMR (400MHz, $CDCl_3$) spectrum of **[(4-methoxyphenyl)ethynyl]trimethylsilane.**

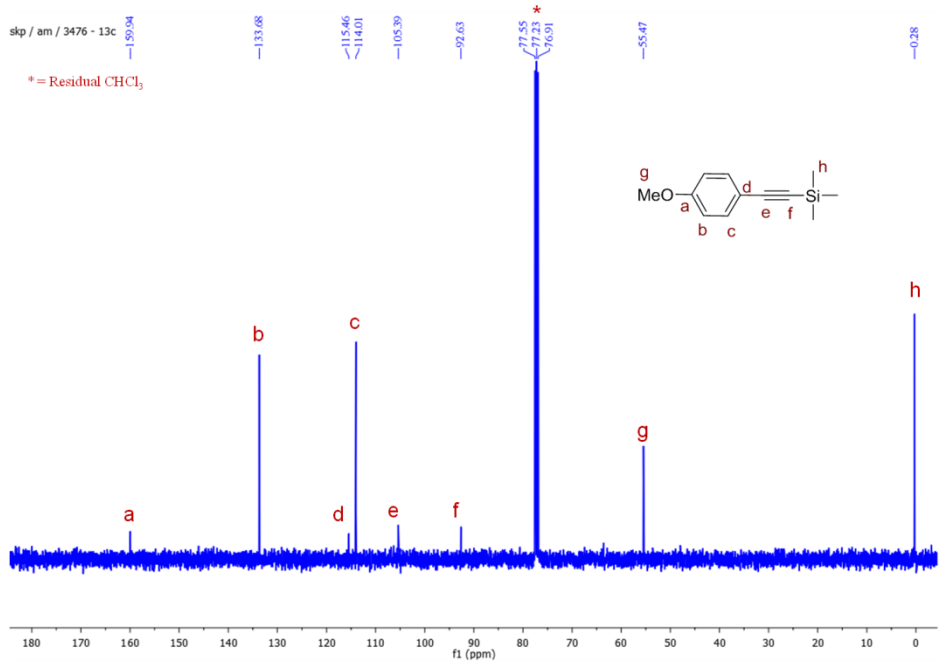

Fig S2: $^{13}C\{^{1}H\}$NMR (100MHz, $CDCl_3$) spectrum of **[(4 methoxyphenyl)ethynyl]trimethyl silane.**

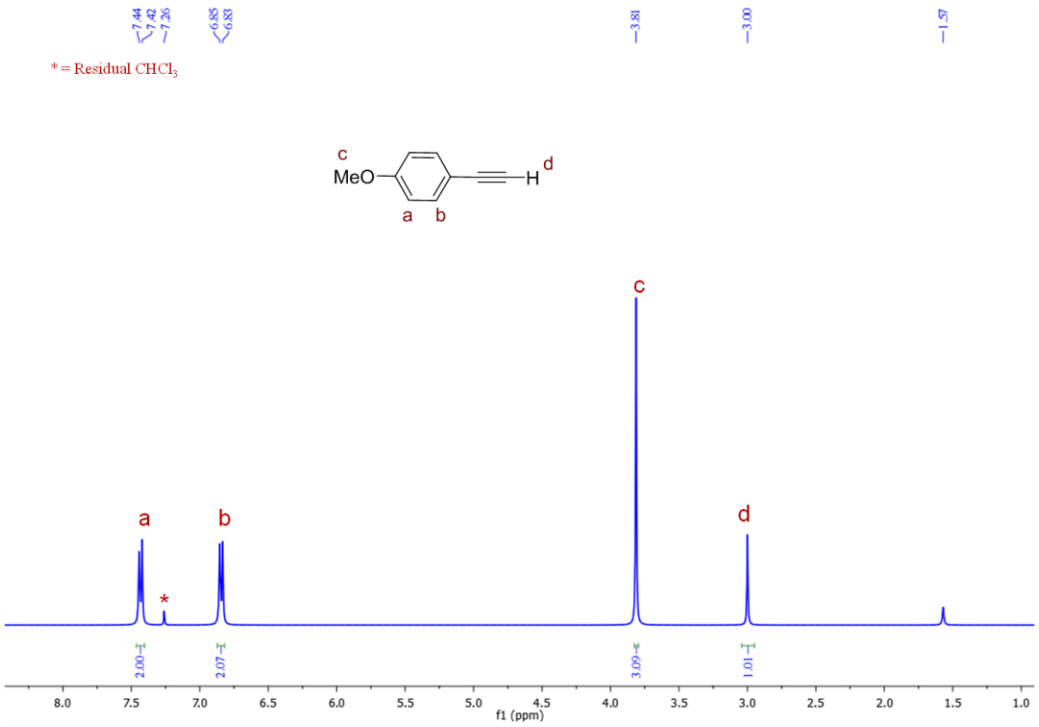

Fig S3: ^{1}H NMR (400MHz, $CDCl_3$) spectrum of **4-Ethynylanisole**

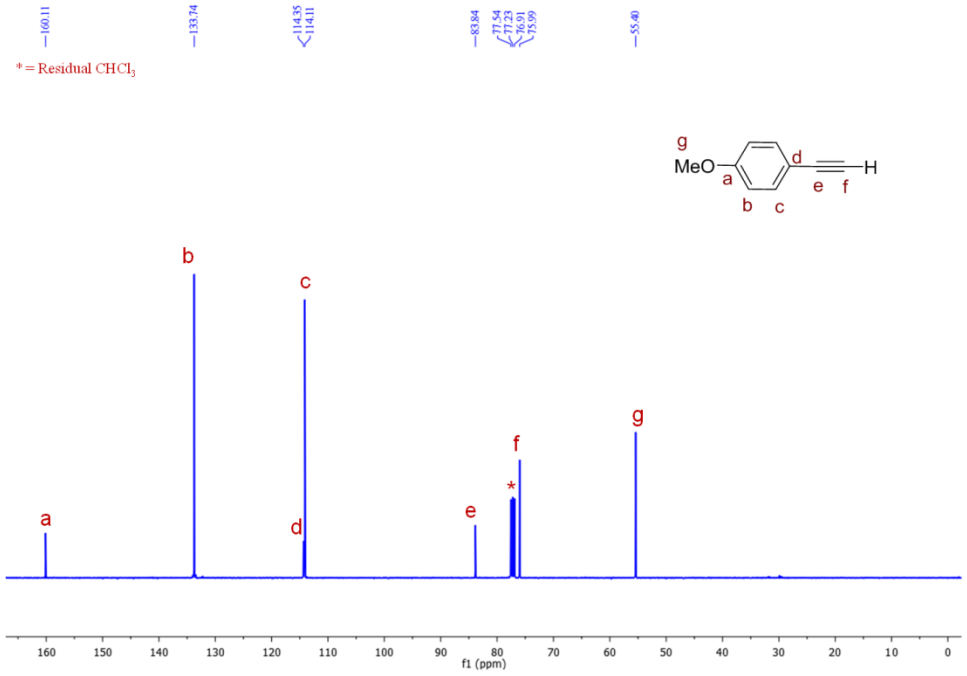

Fig S4: $^{13}C\{^{1}H\}$NMR (100MHz, $CDCl_3$) spectrum of **4-Ethynylanisole**

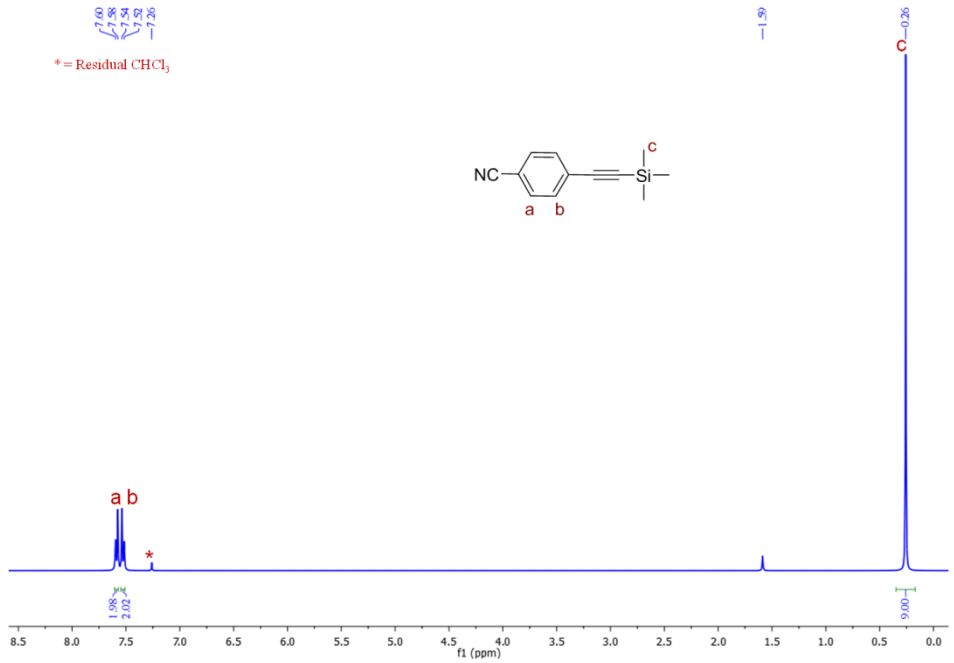

Fig S5: ^{1}H NMR (400MHz, $CDCl_3$) spectrum of **4-[(Trimethylsilyl)ethynyl]benzonitrile**

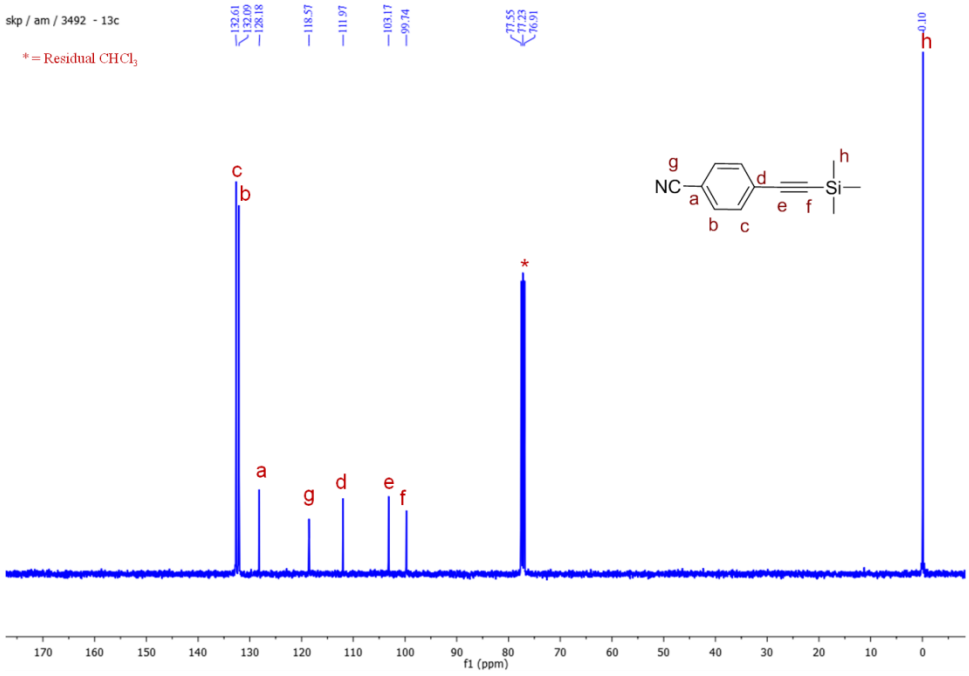

Fig S6: $^{13}C\{^{1}H\}$NMR (100MHz, $CDCl_3$) spectrum of **4-[(Trimethylsilyl)ethynyl]benzonitrile**

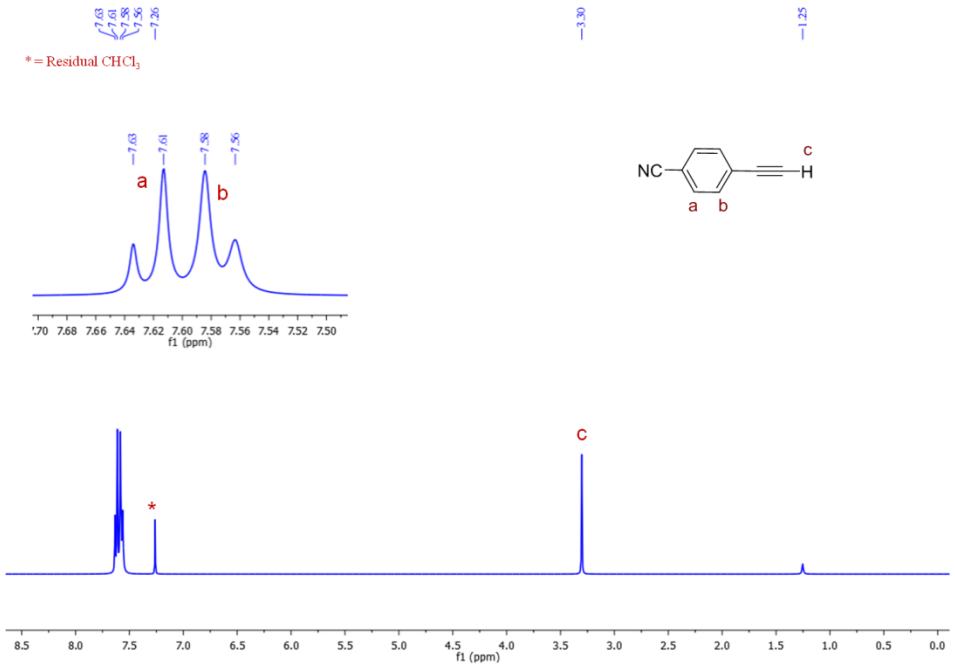

Fig S7: ^{1}H NMR (400MHz, $CDCl_3$) spectrum of **4-Ethynylbenzonitrile**

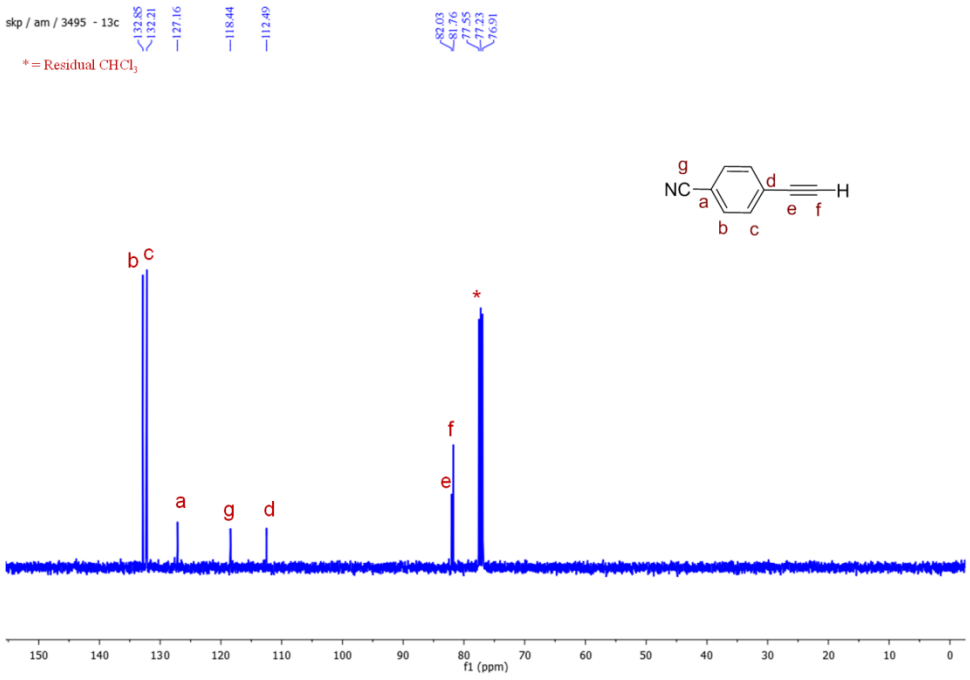

Fig S8: $^{13}C\{^{1}H\}$NMR (100MHz, $CDCl_3$) spectrum of **4-Ethynylbenzonitrile**

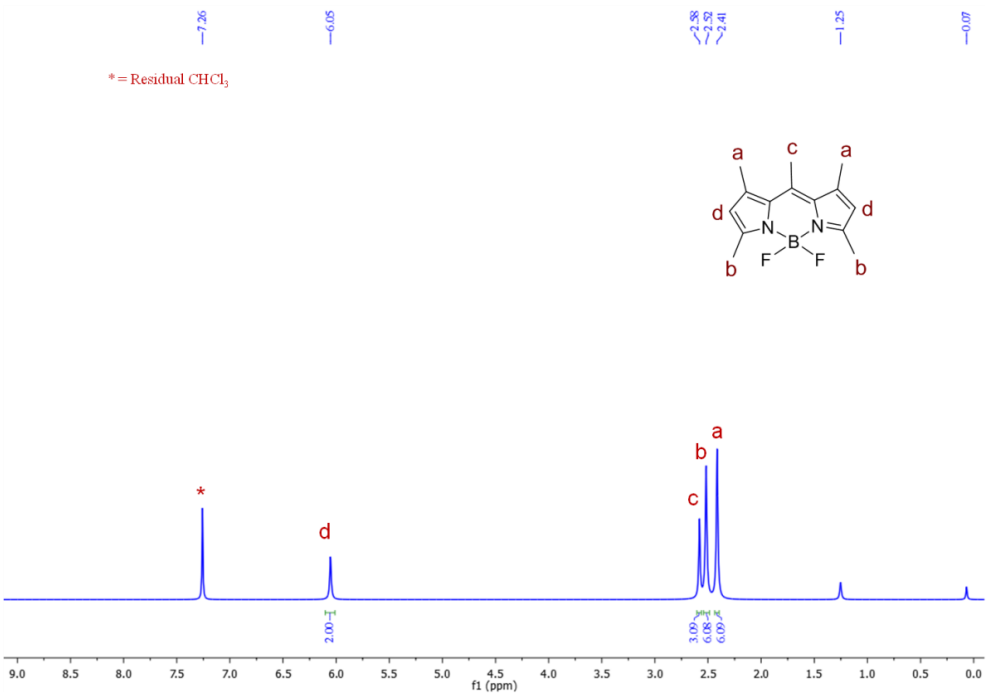

Fig S9: ^{1}H NMR (400MHz, $CDCl_3$) spectrum of **1**

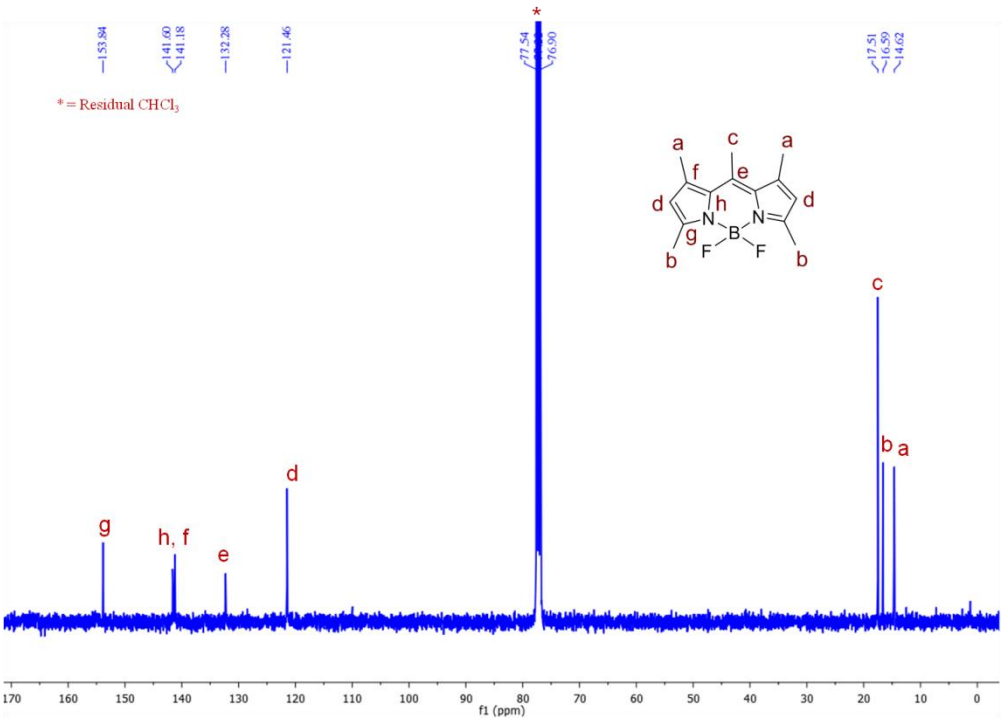

Fig S10: $^{13}C\{^{1}H\}$NMR (100MHz, $CDCl_3$) spectrum of **1**

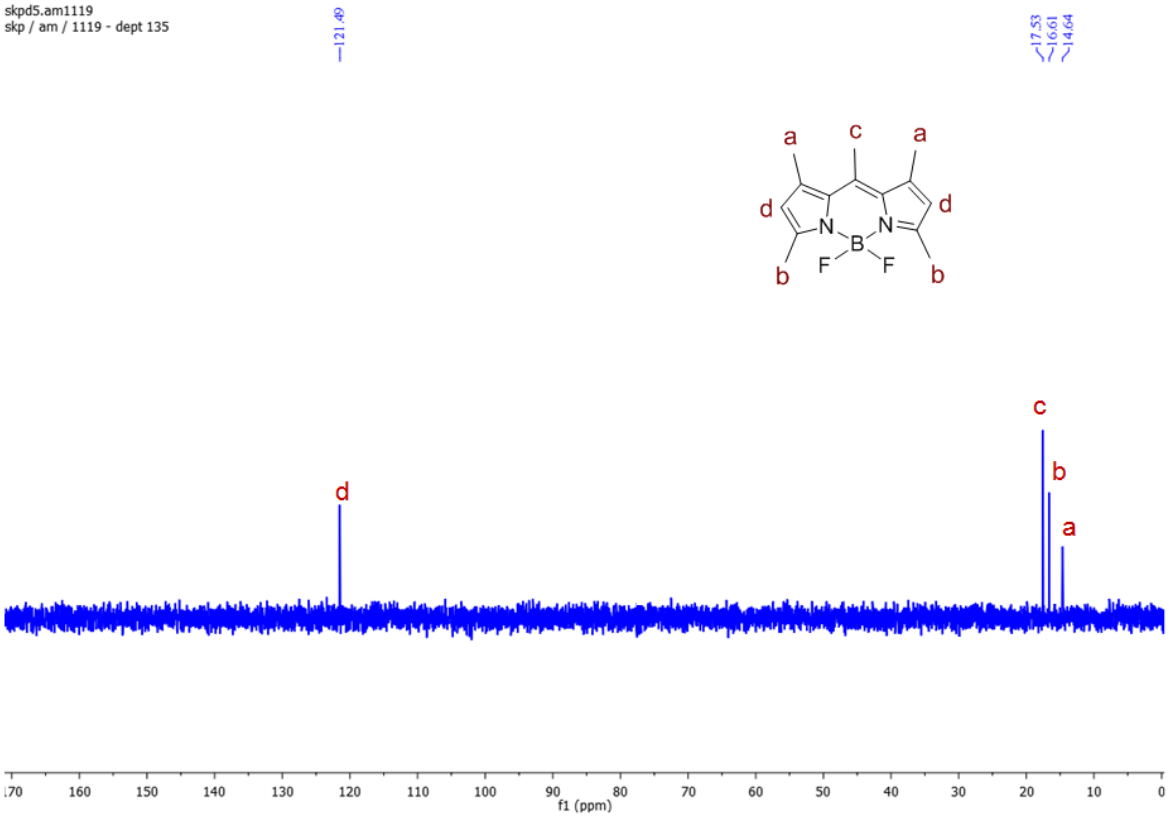

Fig S11: DEPT-135 NMR (100 MHz, $CDCl_3$) spectrum of **1**

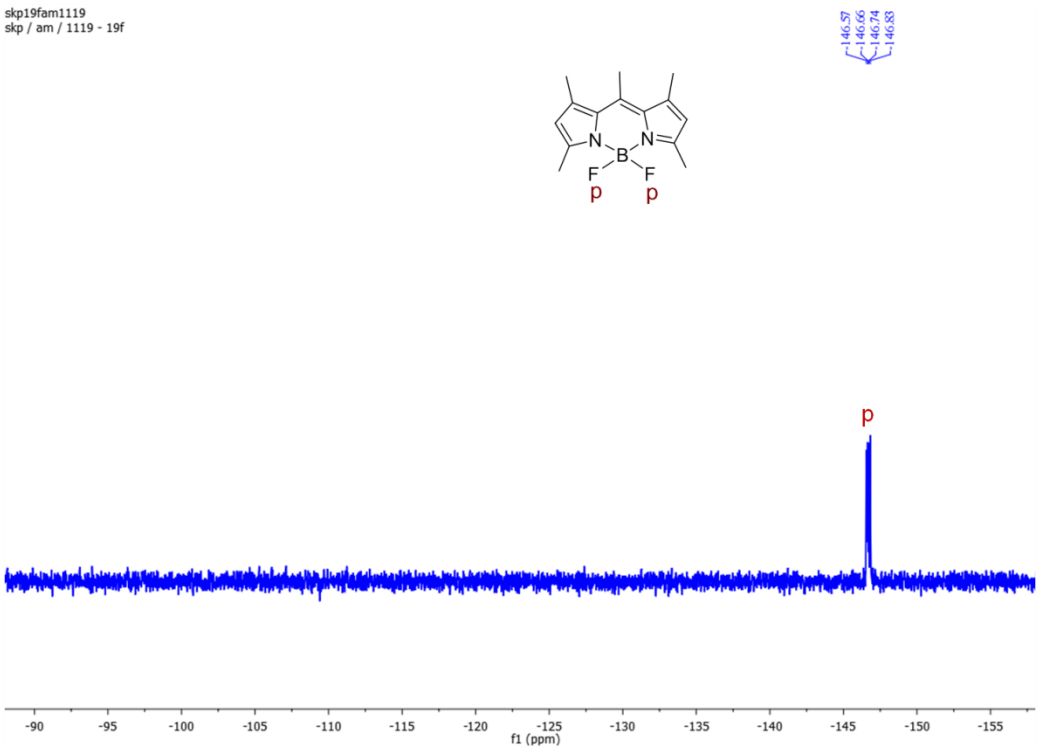

Fig S12: $^{19}F\{^{1}H\}$ NMR (376 MHz, $CDCl_3$) of spectrum **1**

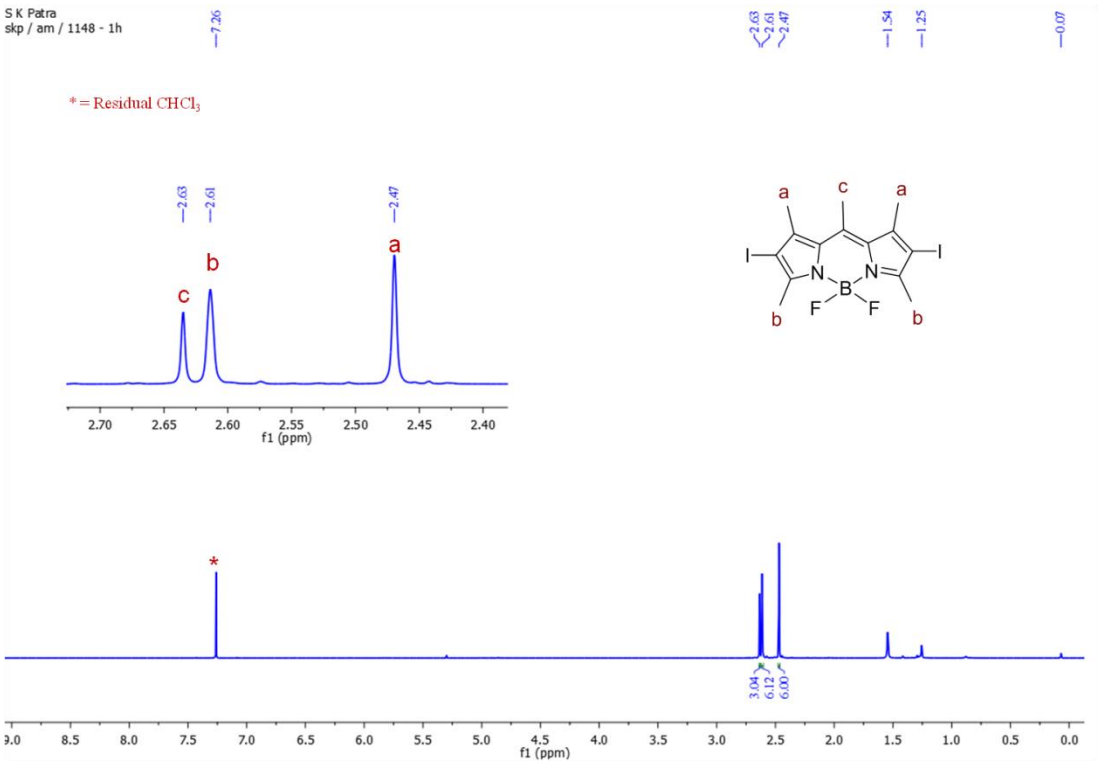

Fig S13: ^{1}H NMR (400 MHz, $CDCl_3$) spectrum of **2**

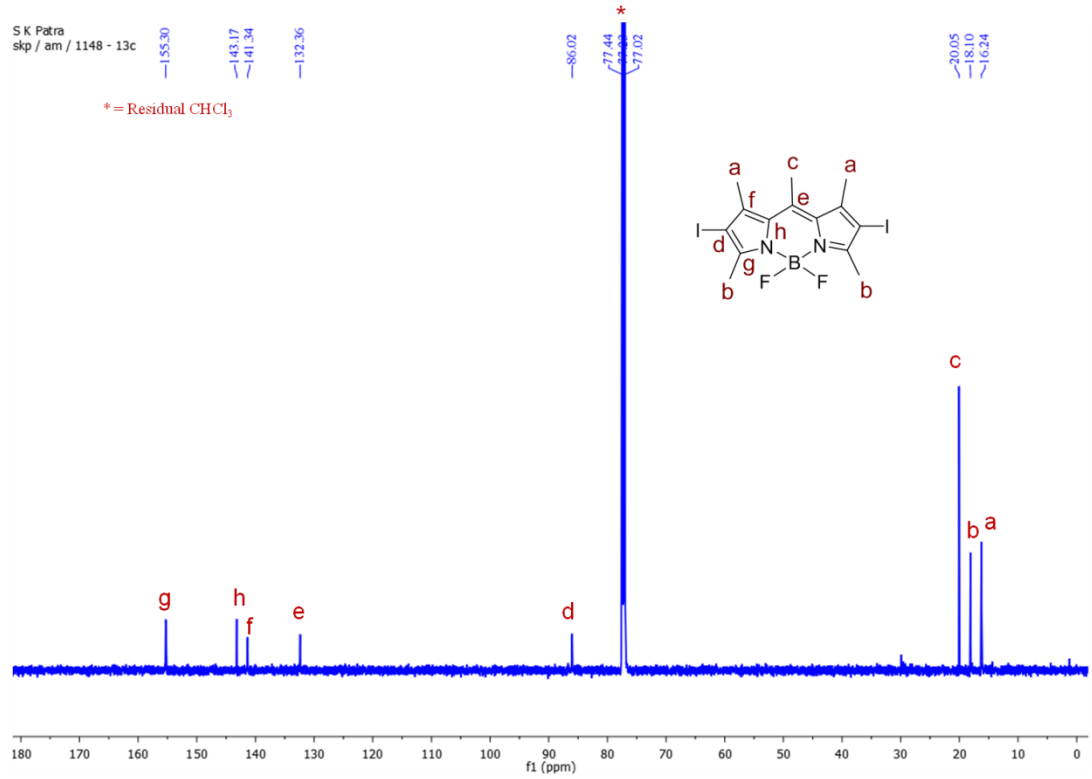

Fig S14: $^{13}C\{^{1}H\}$NMR (100 MHz, $CDCl_3$) spectrum of **2**

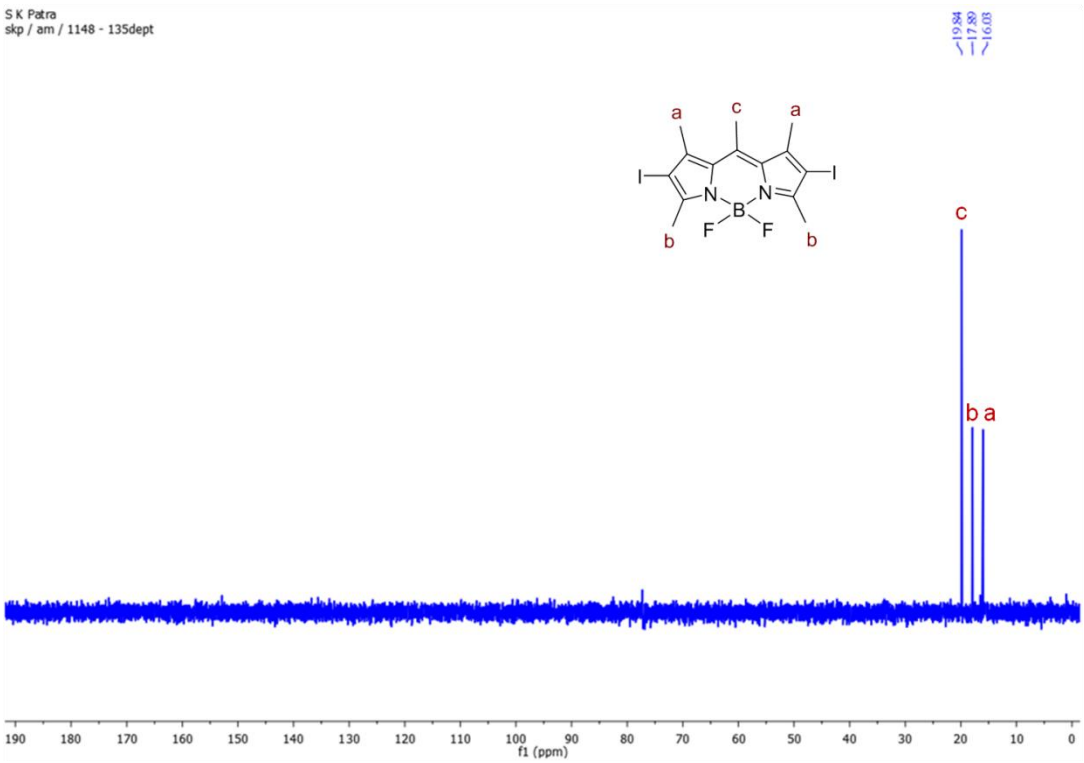

Fig S15: DEPT-135 NMR (100 MHz, $CDCl_3$) spectrum of **2**

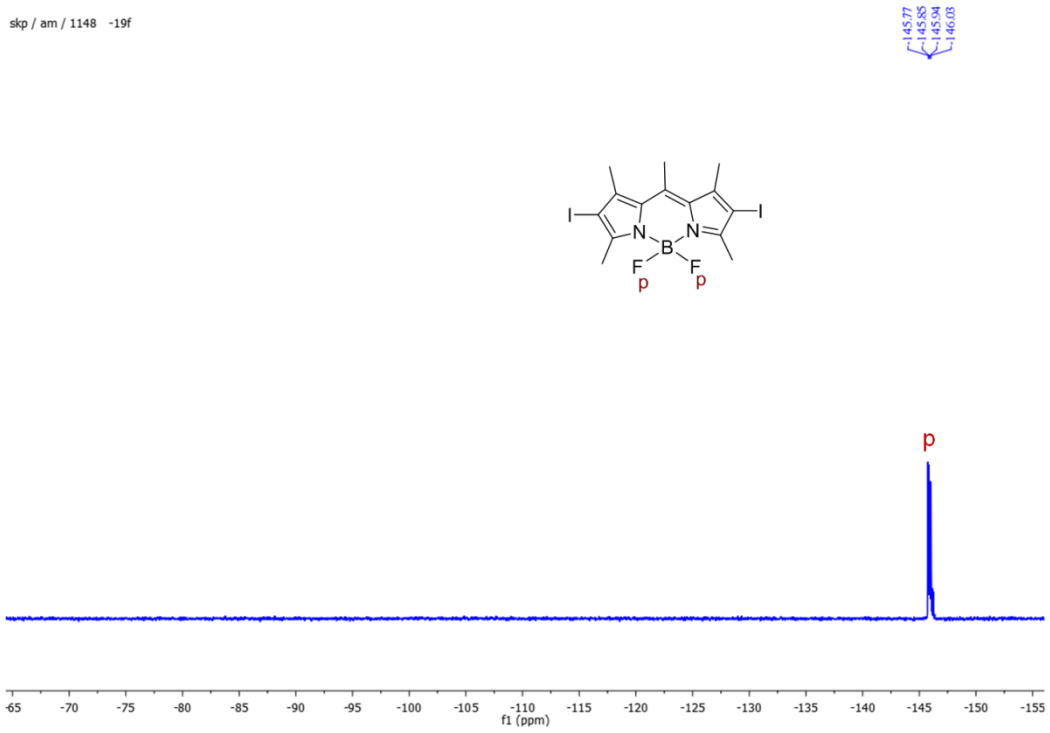

Fig S16: $^{19}F\{H\}$ NMR (376 MHz, $CDCl_3$) spectrum of **2**

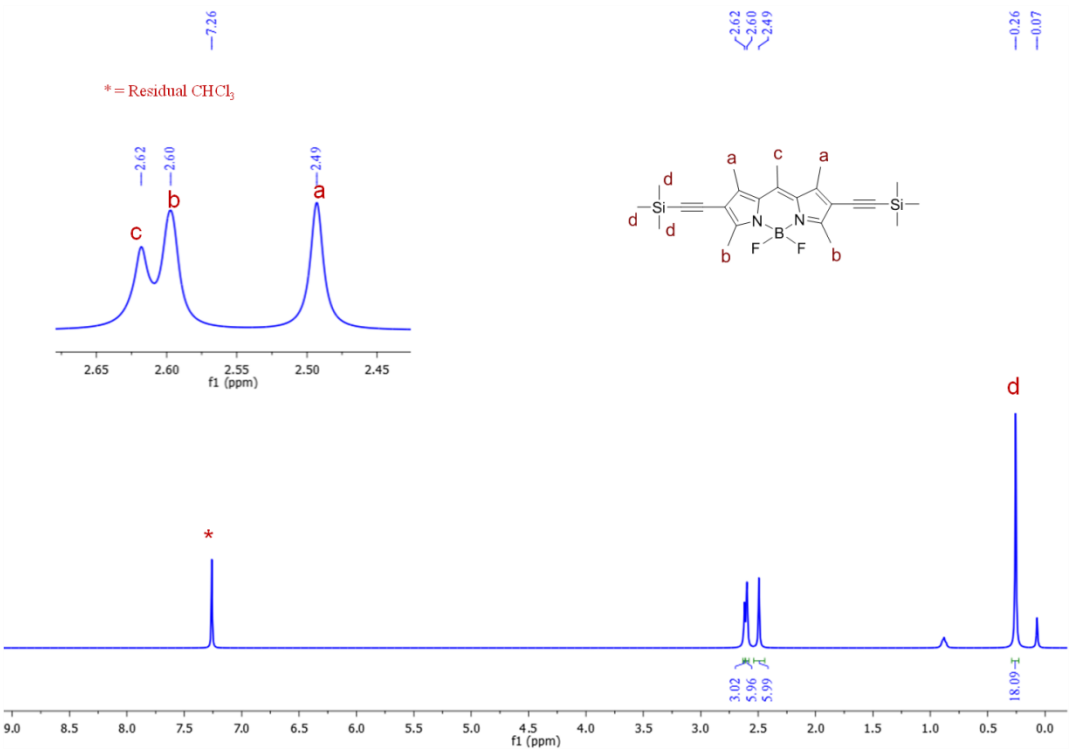

Fig S17: ^{1}H NMR (400MHz, $CDCl_3$) spectrum of **3**

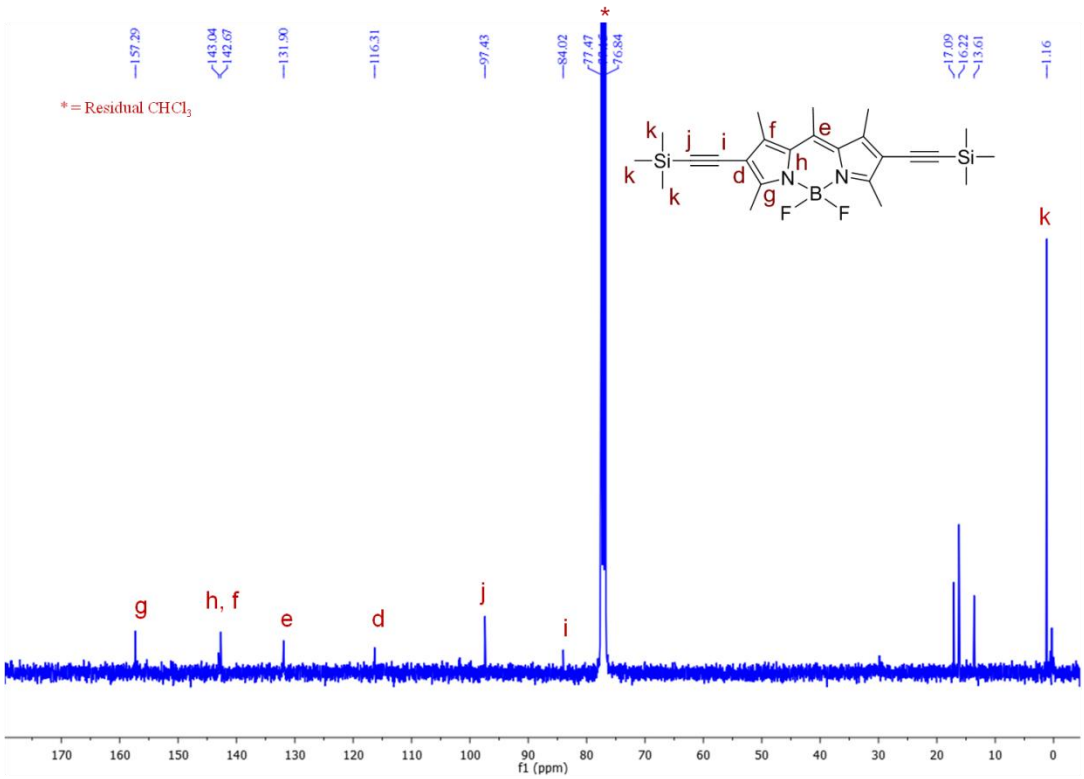

Fig S18: ^{13}C{^{1}H}NMR (100 MHz, $CDCl_3$) spectrum of **3**

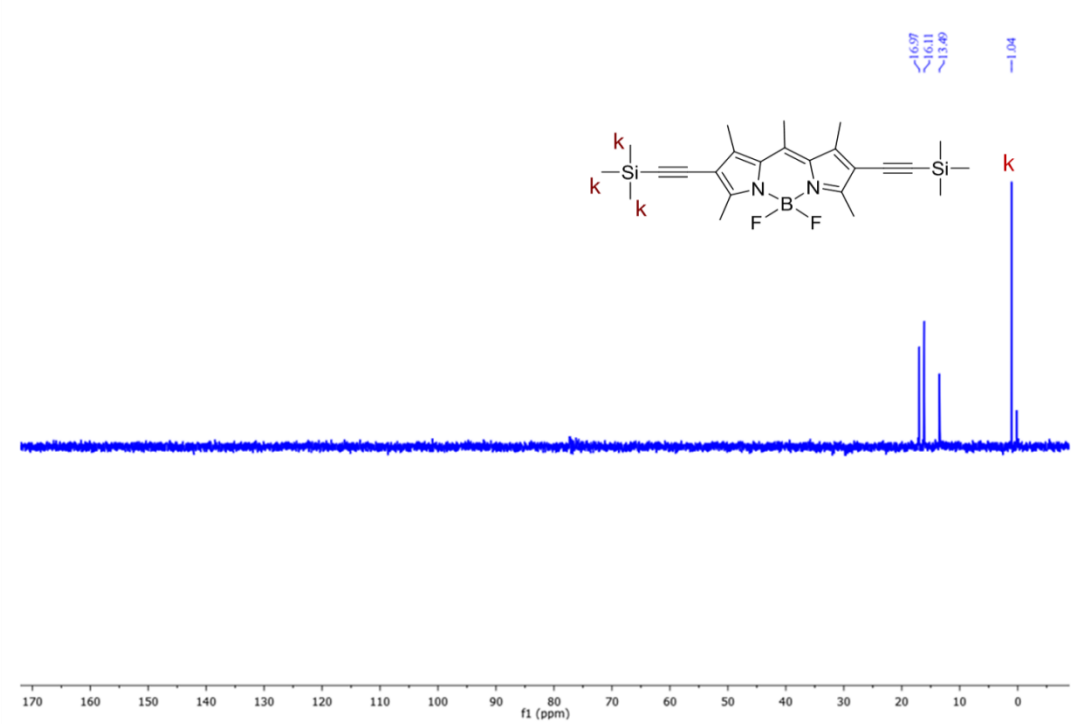

Fig S19: DEPT-135 NMR (100 MHz, $CDCl_3$) spectrum of **3**

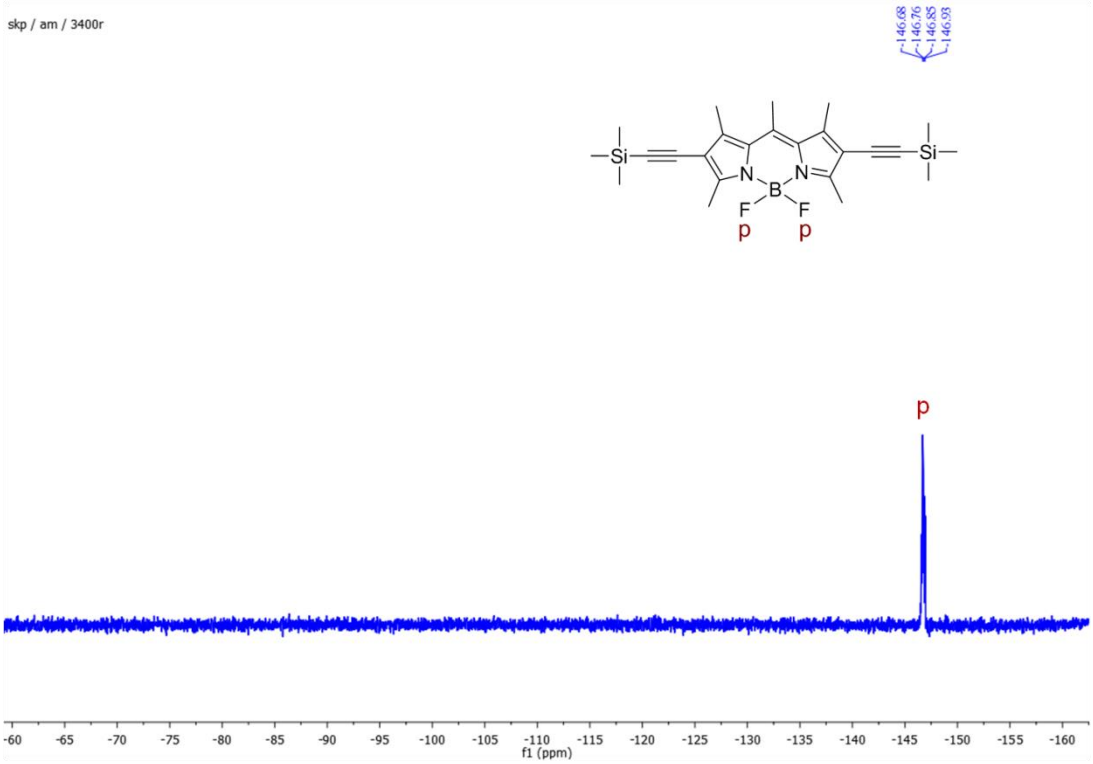

Fig S20: $^{19}F\{^1H\}$ NMR (376 MHz, $CDCl_3$) spectrum of **3**

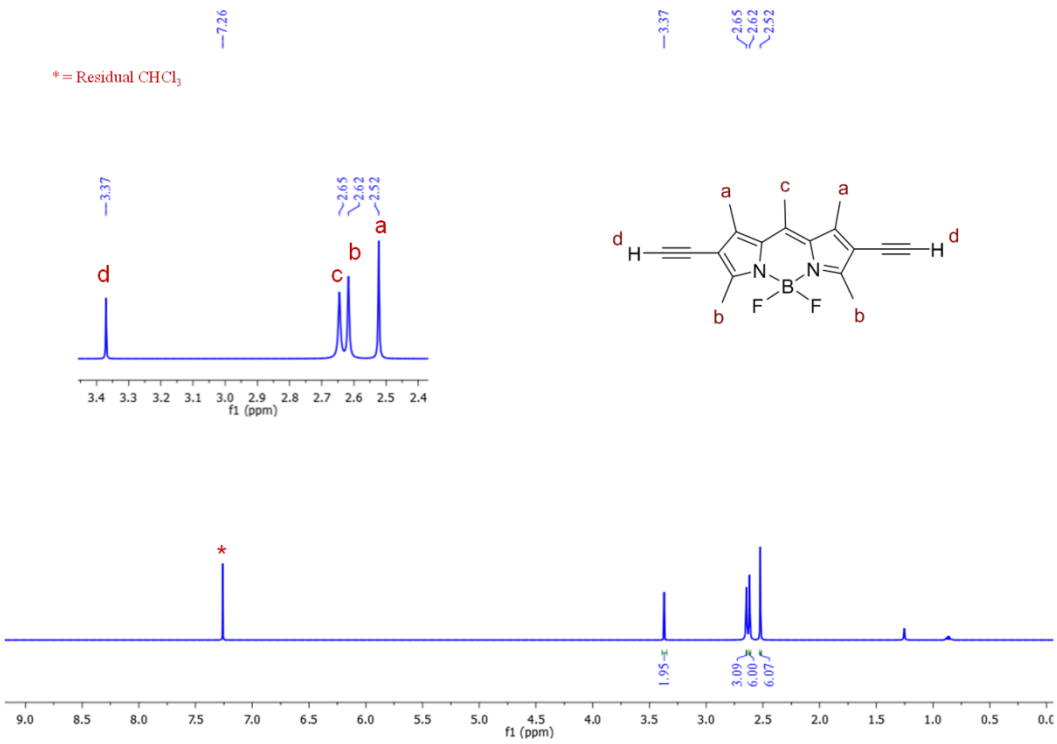

Fig S21: ^{1}H NMR (600 MHz, $CDCl_3$) spectrum of **PBDP1**

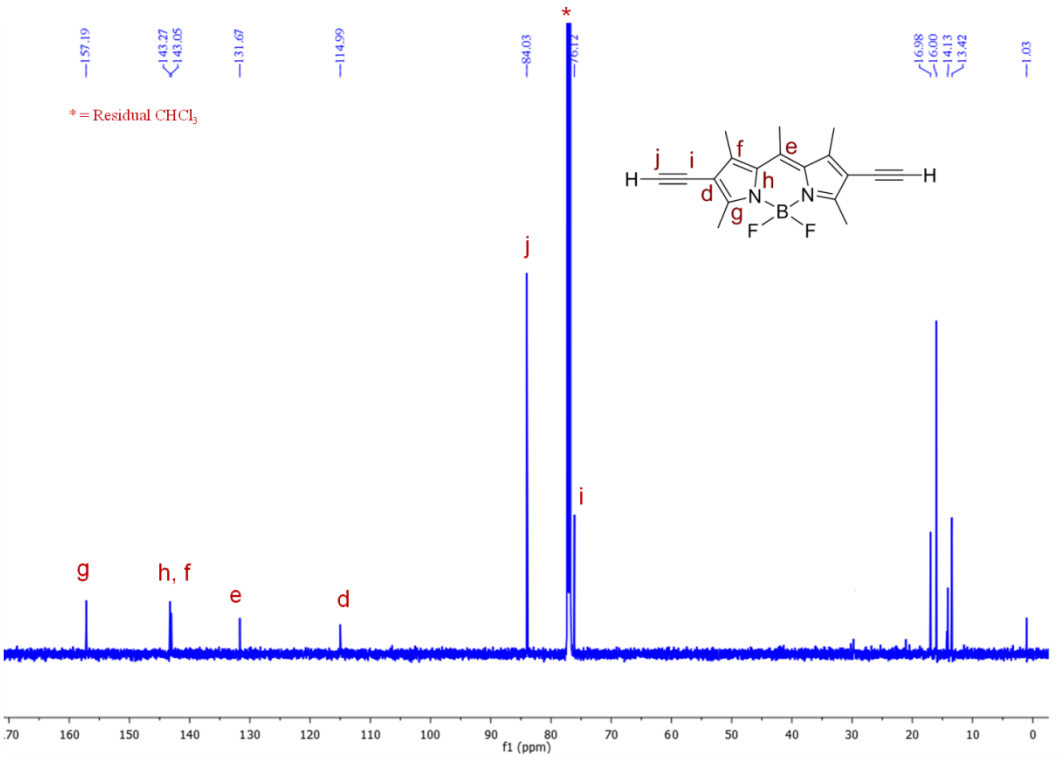

Fig S22: $^{13}C\{^{1}H\}$ NMR (150 MHz, $CDCl_3$) spectrum of **PBDP1**

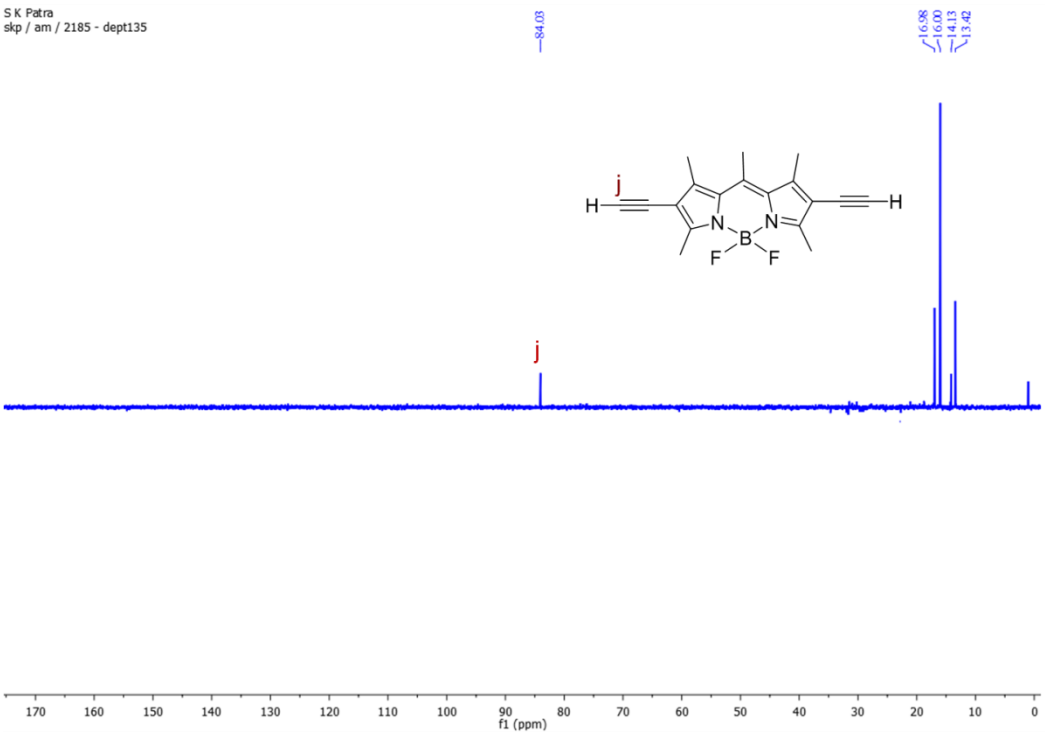

Fig S23: DEPT-135 NMR (150 MHz, $CDCl_3$) spectrum of **PBDP1**

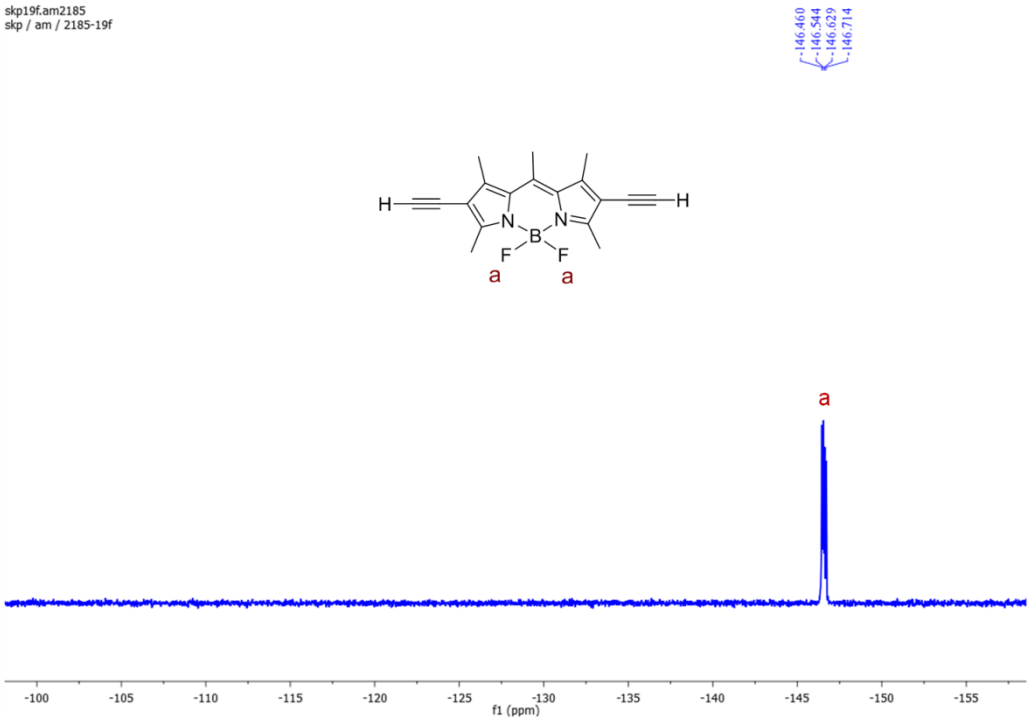

Fig S24: $^{19}F\{^{1}H\}$ NMR (376 MHz, $CDCl_3$) spectrum of **PBDP1**

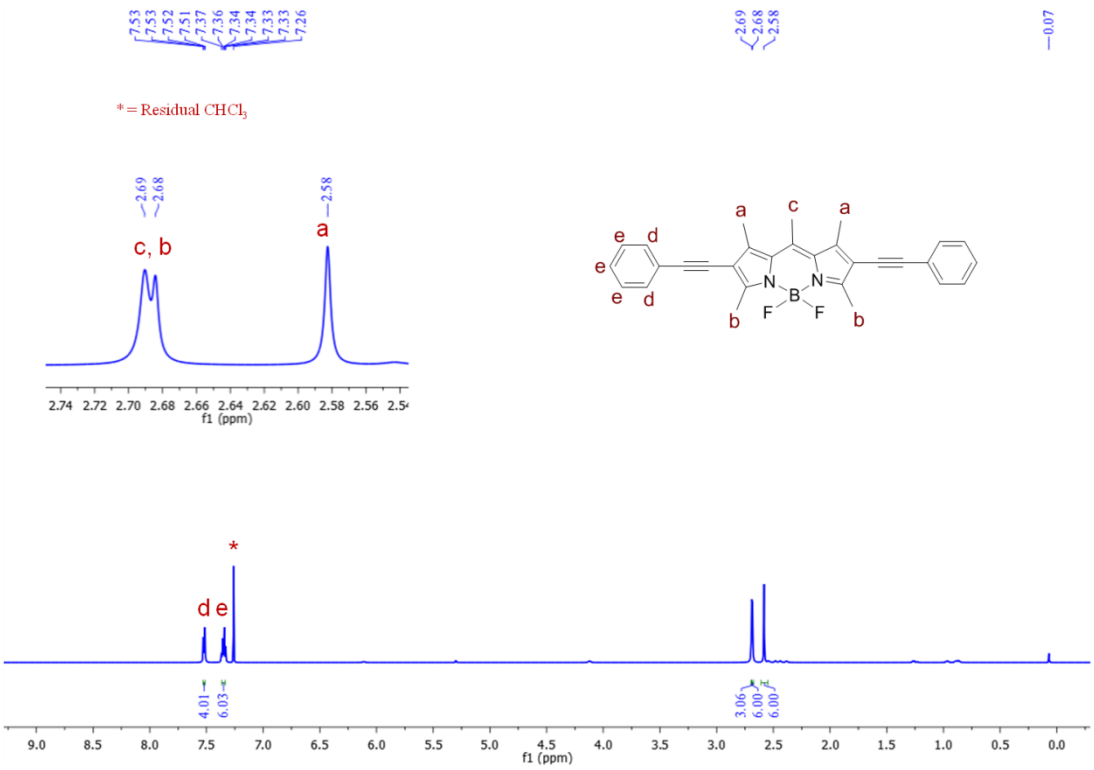

Fig S25: ^{1}H NMR (600 MHz, $CDCl_3$) spectrum of **PBDP2**

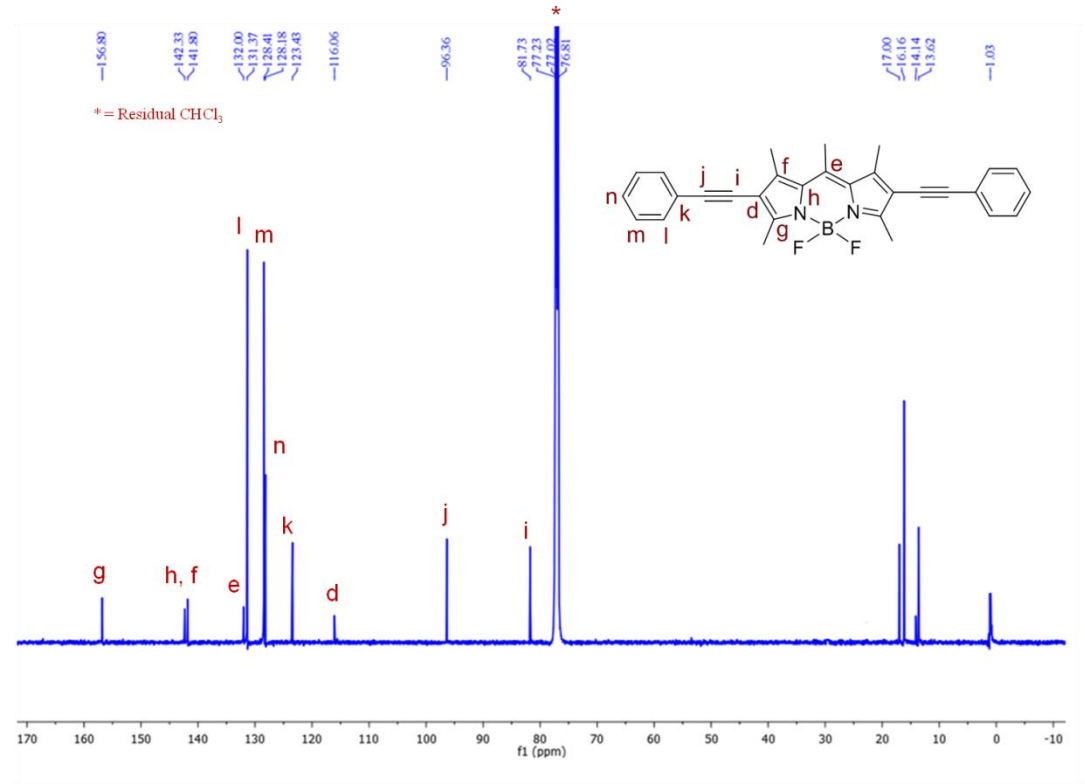

Fig S26: $^{13}C\{^{1}H\}$ NMR (150 MHz, $CDCl_3$) spectrum of **PBDP2**

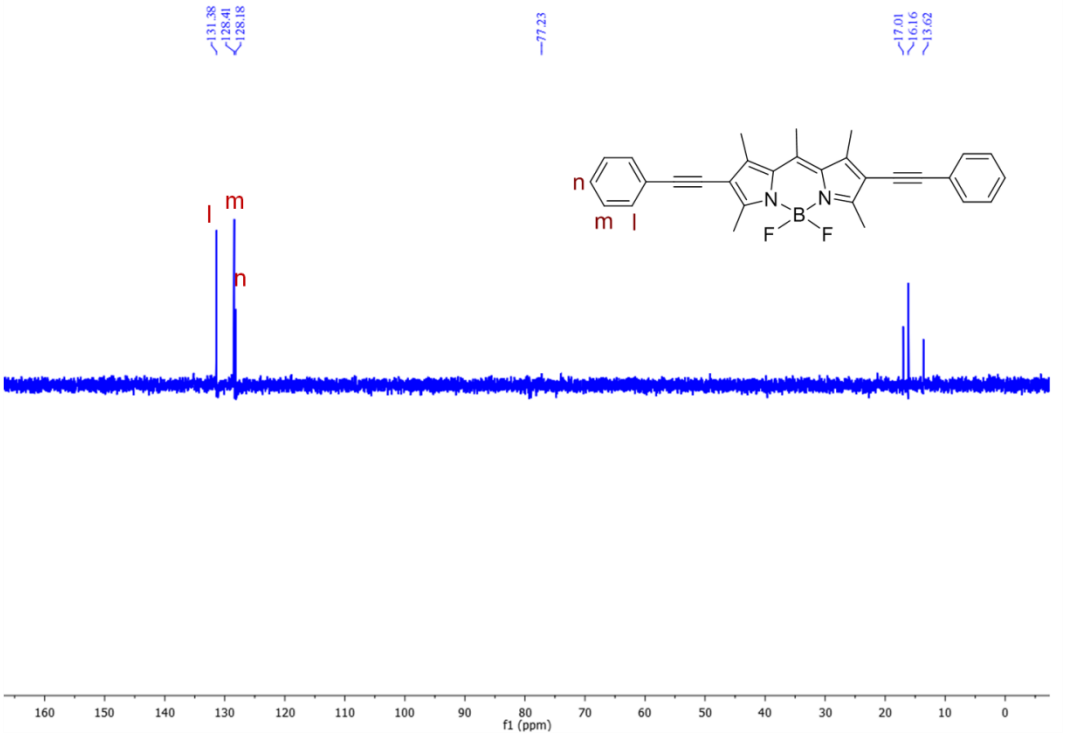

Fig S27: DEPT-135 NMR (150 MHz, $CDCl_3$) spectrum of **PBDP2**

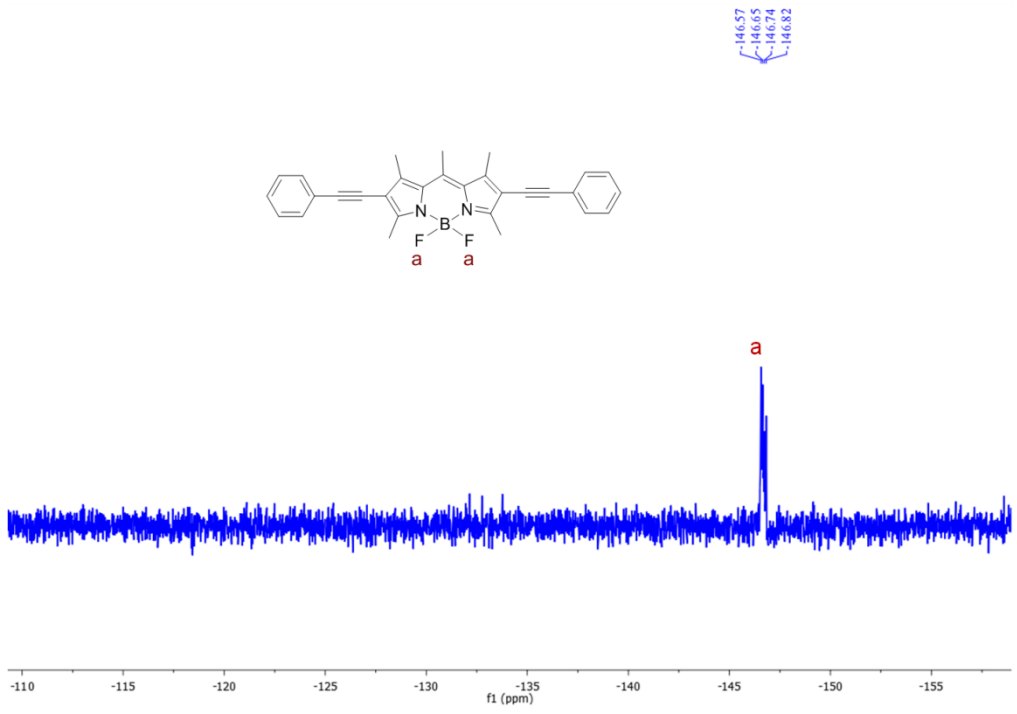

Fig S28: $^{19}F\{^1H\}$ NMR (376 MHz, $CDCl_3$) of **PBDP2**

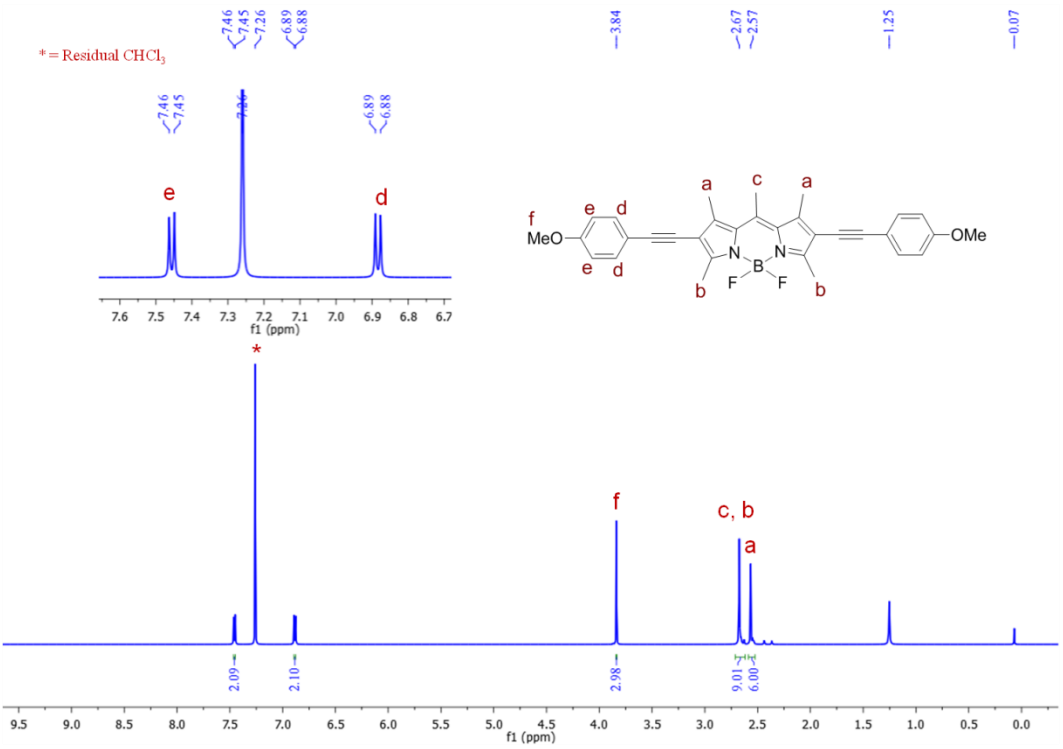

Fig S29: ^{1}H NMR (600 MHz, $CDCl_3$) spectrum of **PBDP3**

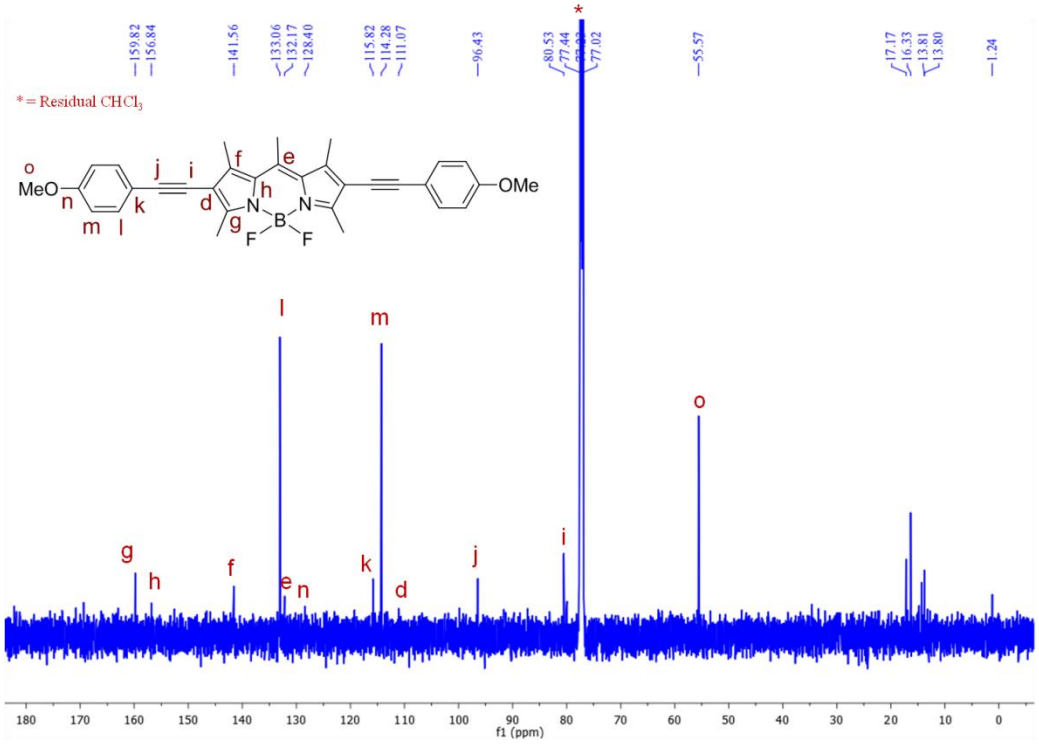

Fig S30: ^{13}C{^{1}H} NMR (150 MHz, $CDCl_3$) spectrum of **PBDP3**

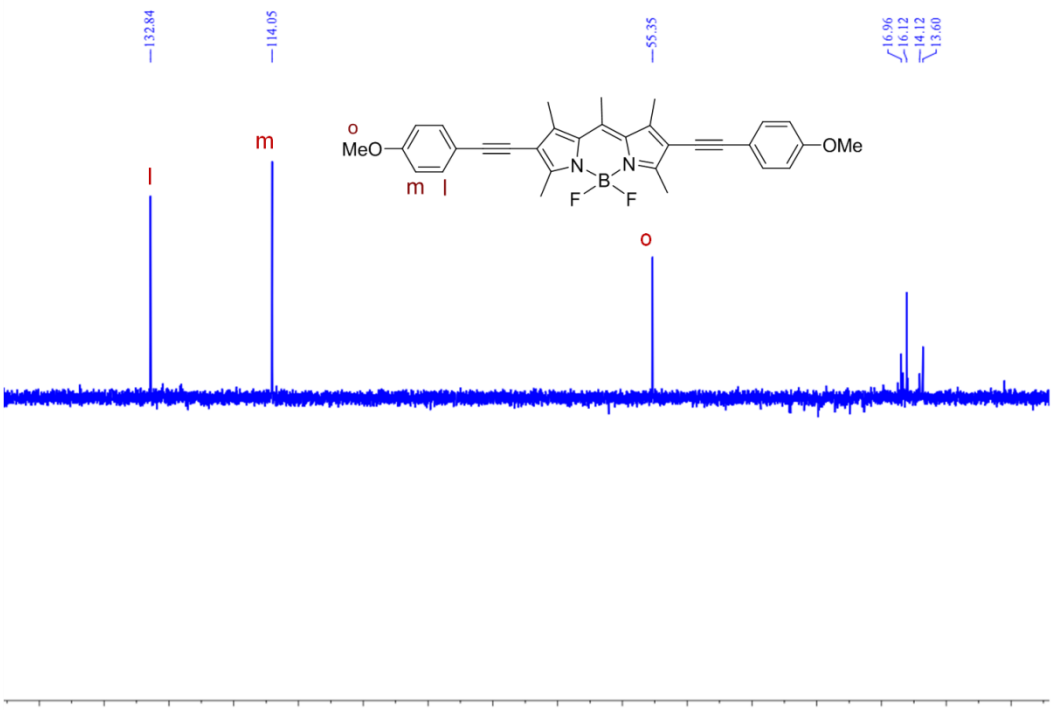

Fig S31: DEPT-135 NMR (150 MHz, $CDCl_3$) spectrum of **PBDP3**

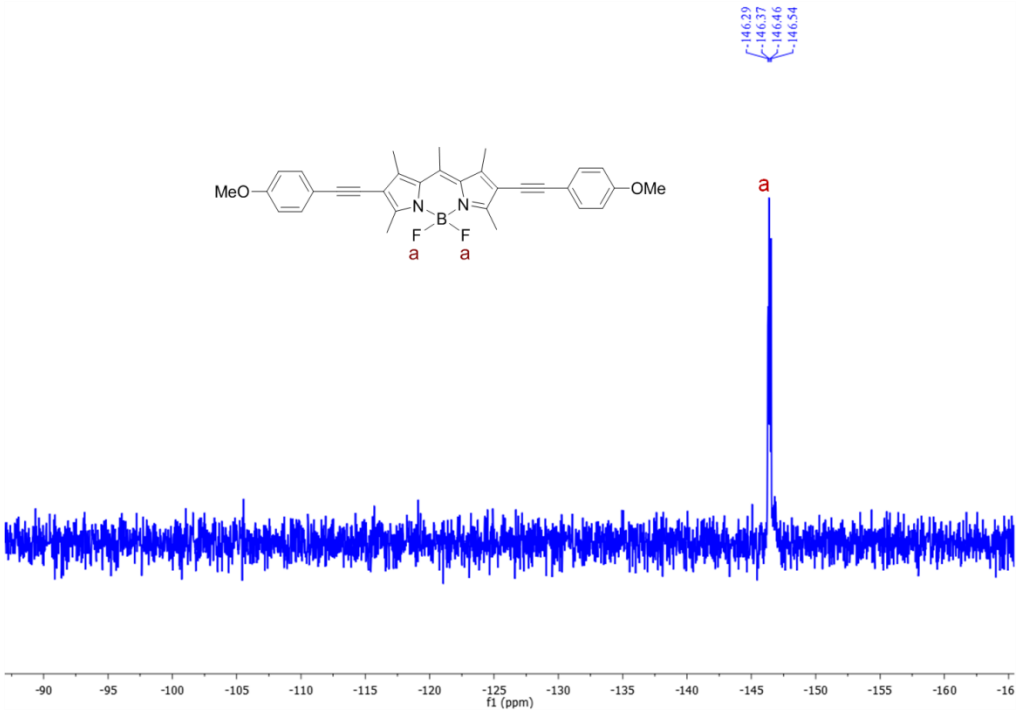

Fig S32: $^{19}F\{^{1}H\}$ NMR (376 MHz, $CDCl_3$) spectrum of **PBDP3**

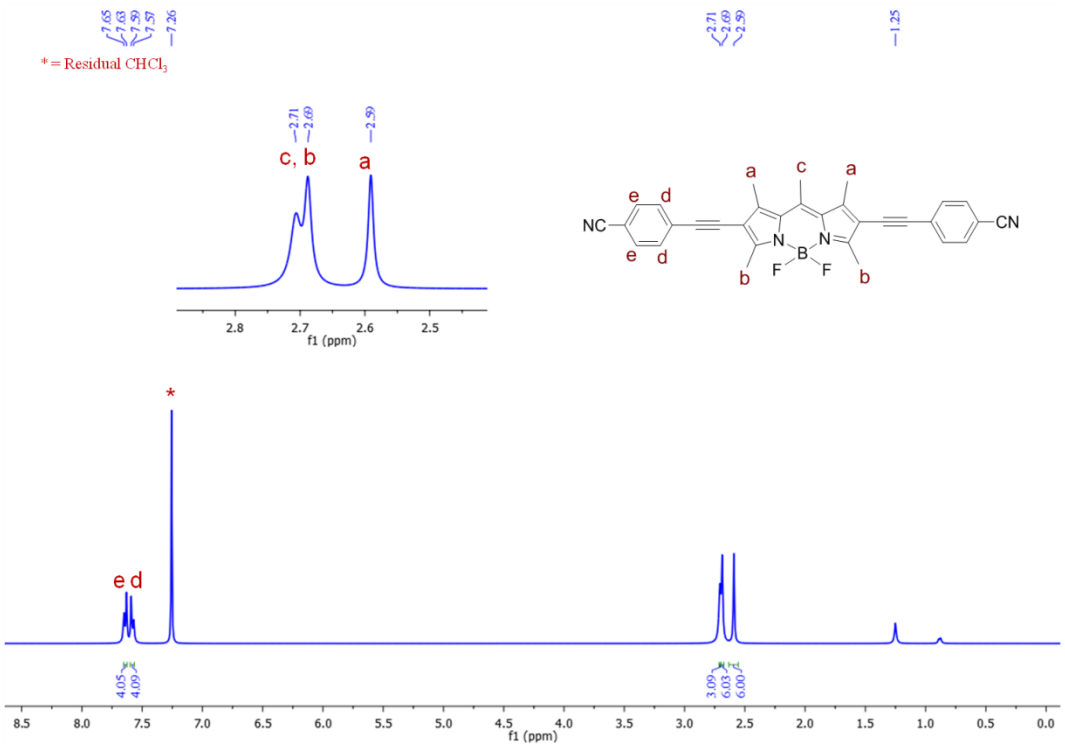

Fig S33: ^{1}H NMR (400 MHz, $CDCl_3$) spectrum of **PBDP4**

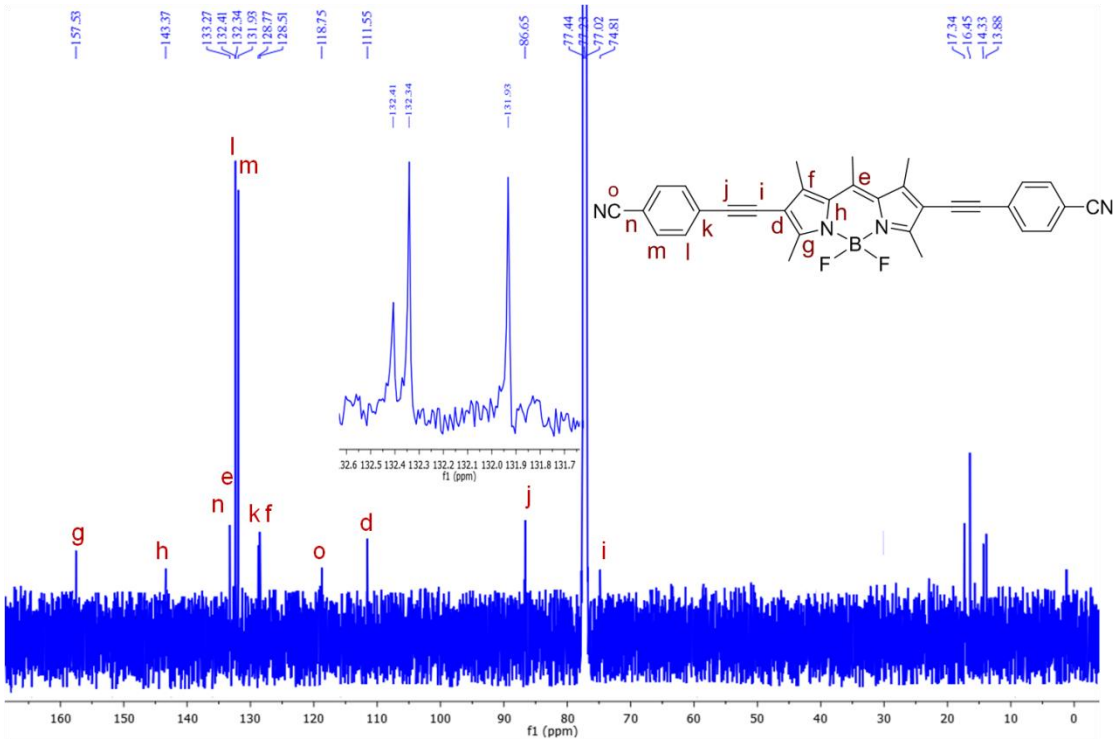

Fig S34: ^{13}C{^{1}H} NMR (150 MHz, $CDCl_3$) spectrum of **PBDP4**

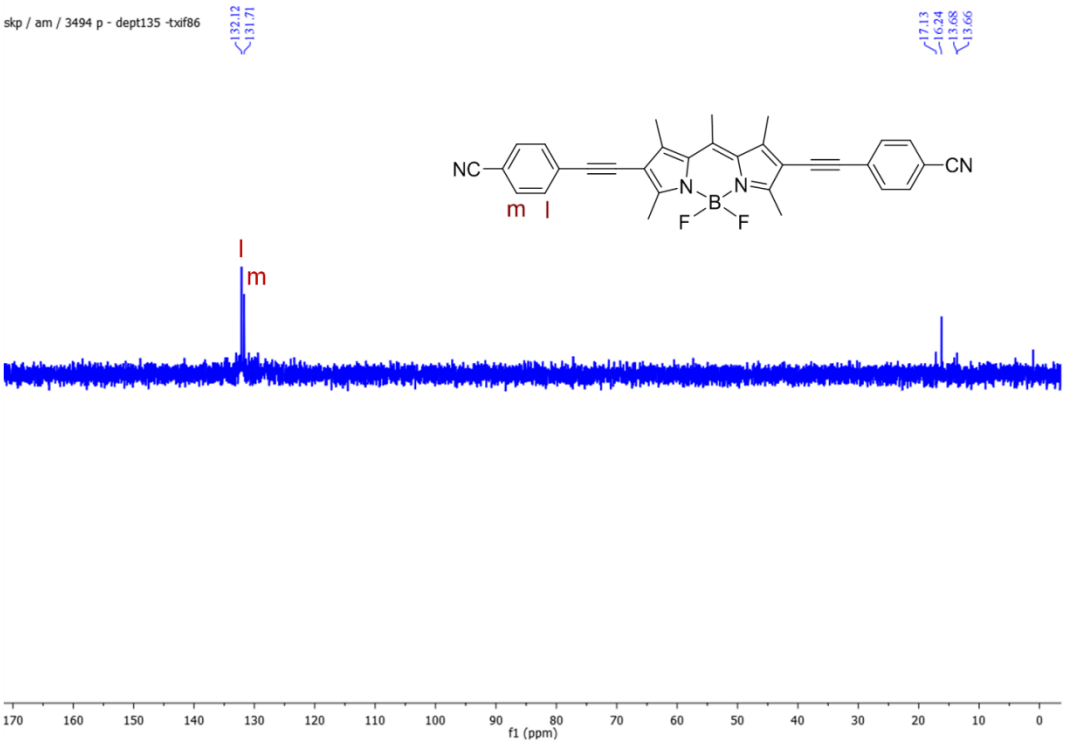

Fig S35: DEPT-135 NMR (150 MHz, $CDCl_3$) spectrum of **PBDP4**

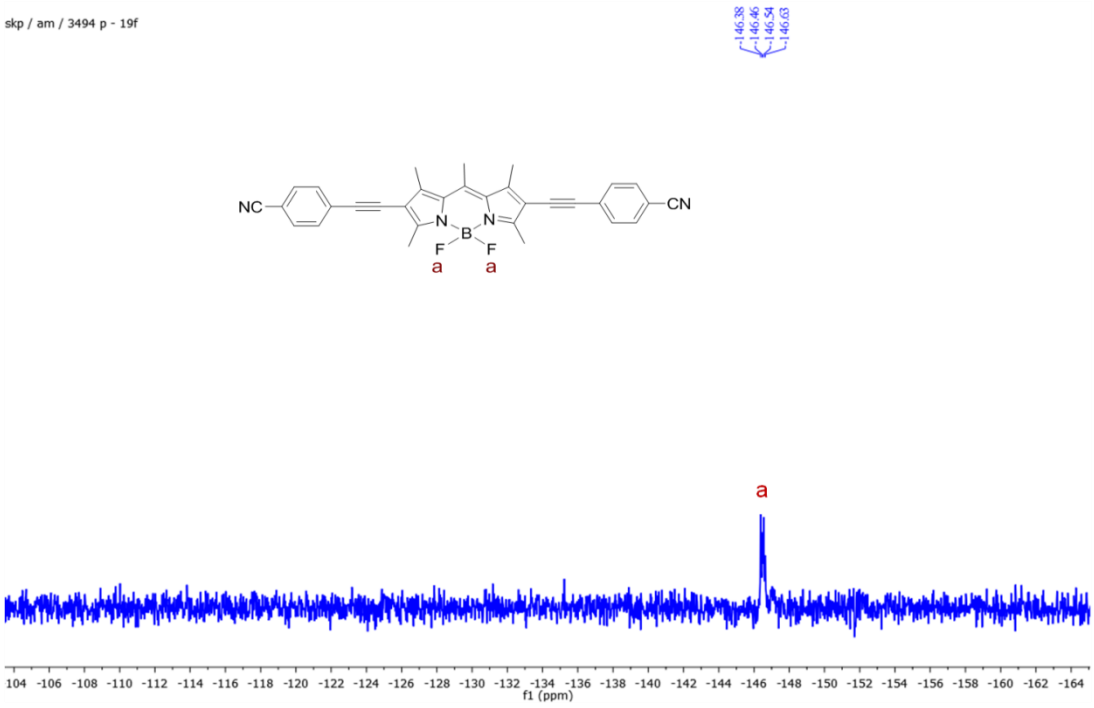

Fig S36: $^{19}F\{^{1}H\}$ NMR (376 MHz, $CDCl_3$) spectrum of **PBDP4**

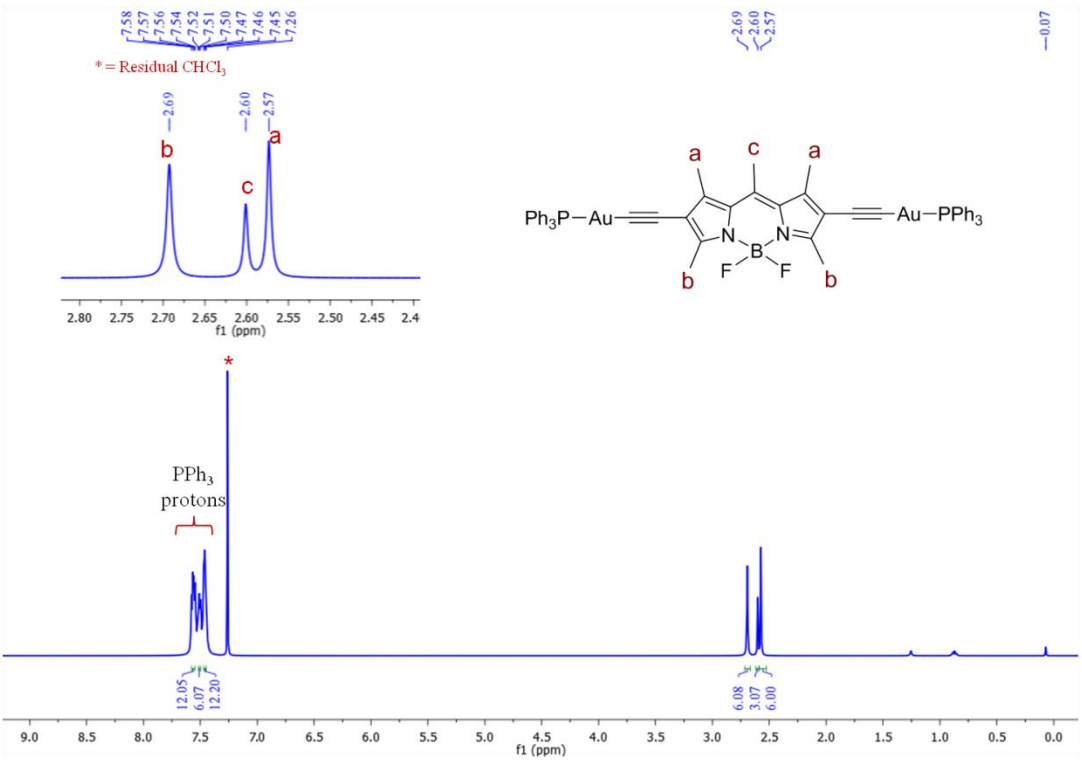

Fig S37: ^{1}H NMR (600 MHz, $CDCl_3$) spectrum of **PBDP5**

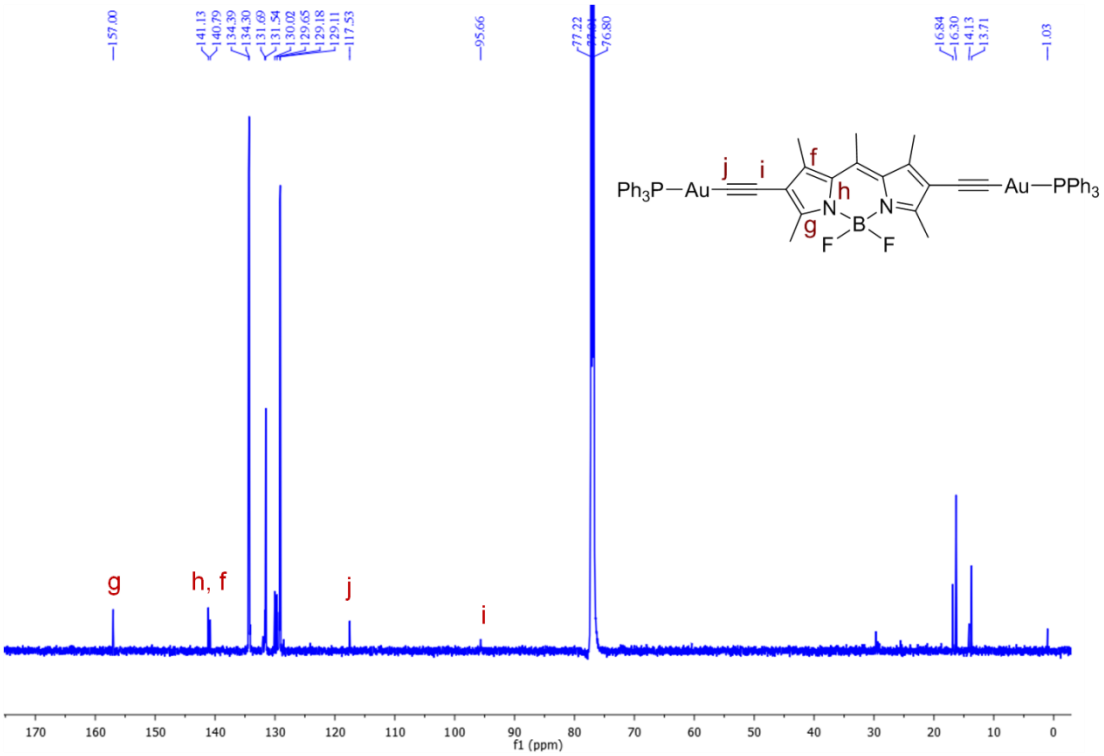

Fig S38: $^{13}C\{^{1}H\}$ NMR (150MHz, $CDCl_3$) spectrum of **PBDP5**

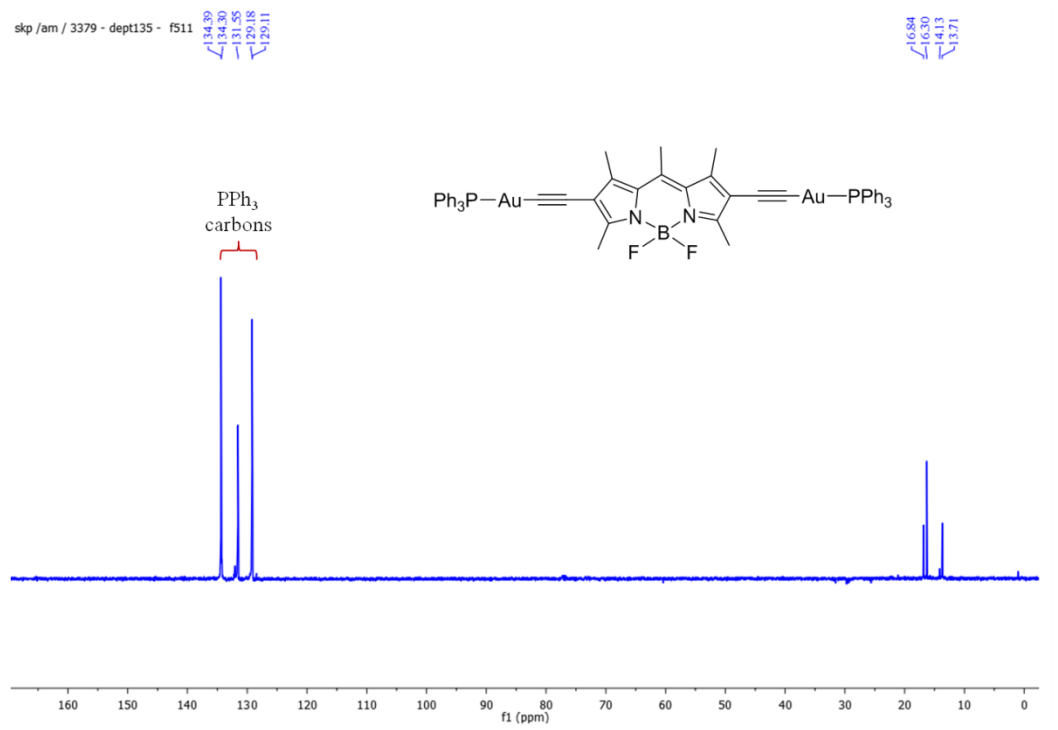

Fig S39: DEPT-135 NMR (150 MHz, $CDCl_3$) spectrum of **PBDP5**

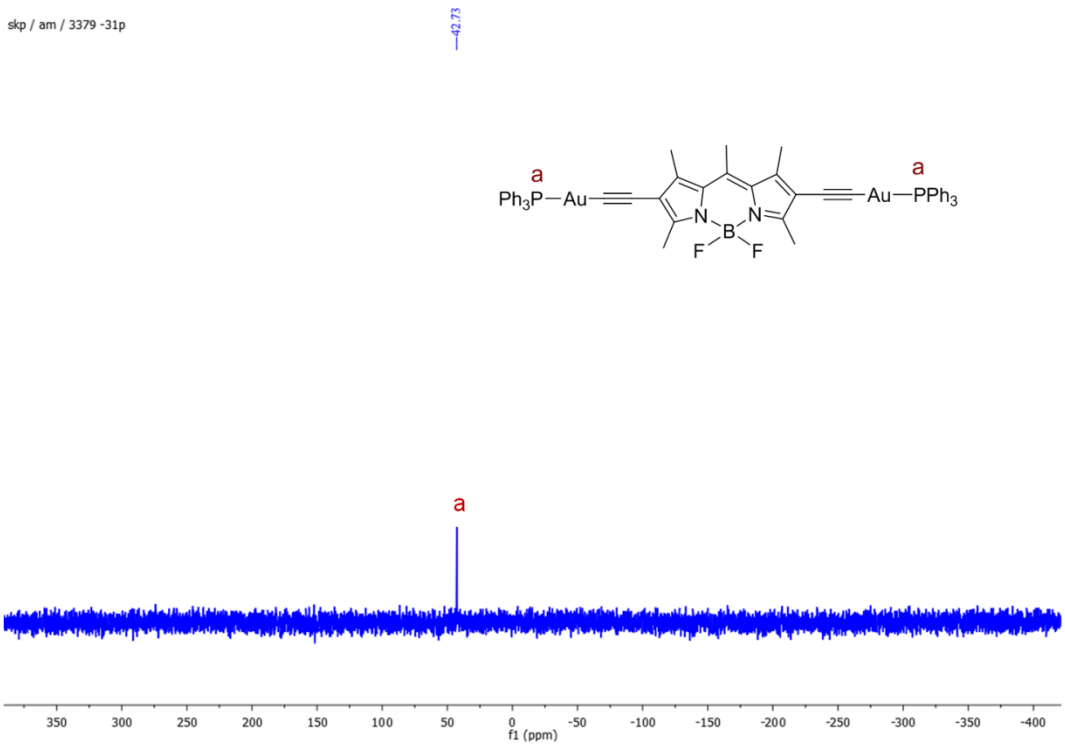

Fig S40: $^{31}P\{^{1}H\}$ NMR (162 MHz, $CDCl_3$) spectrum of **PBDP5**

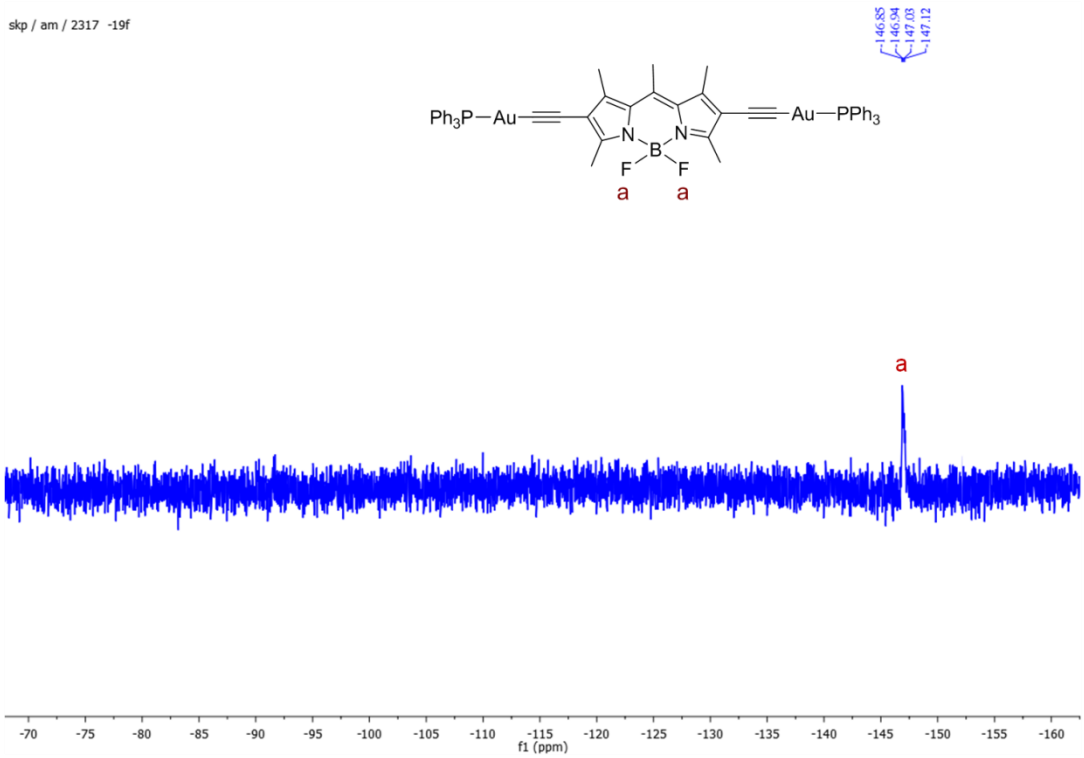

Fig S41: $^{19}F\{^{1}H\}$ NMR (376 MHz, $CDCl_3$) spectrum of **PBDP5**

1c. FTIR Spectra

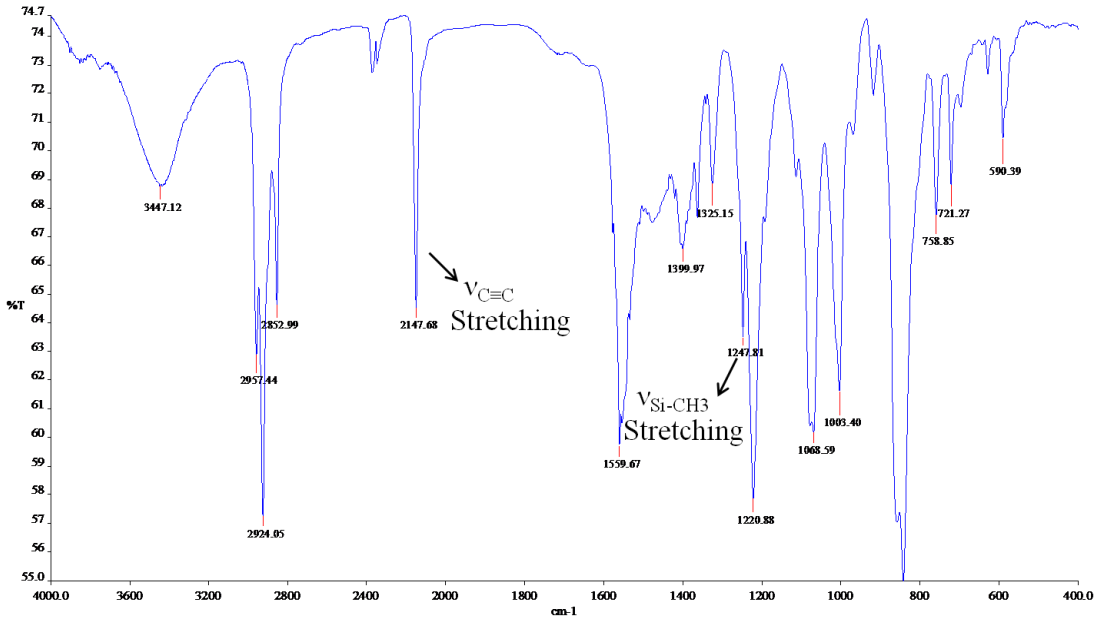

Figure S42. FTIR spectrum of **3**

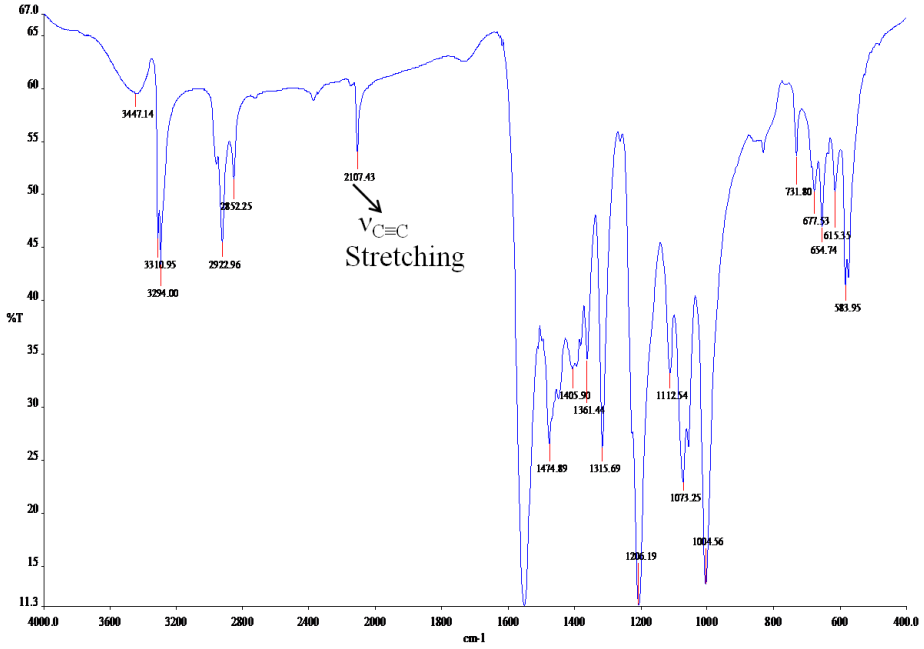

Figure S43. FTIR spectrum of **PBDP1**

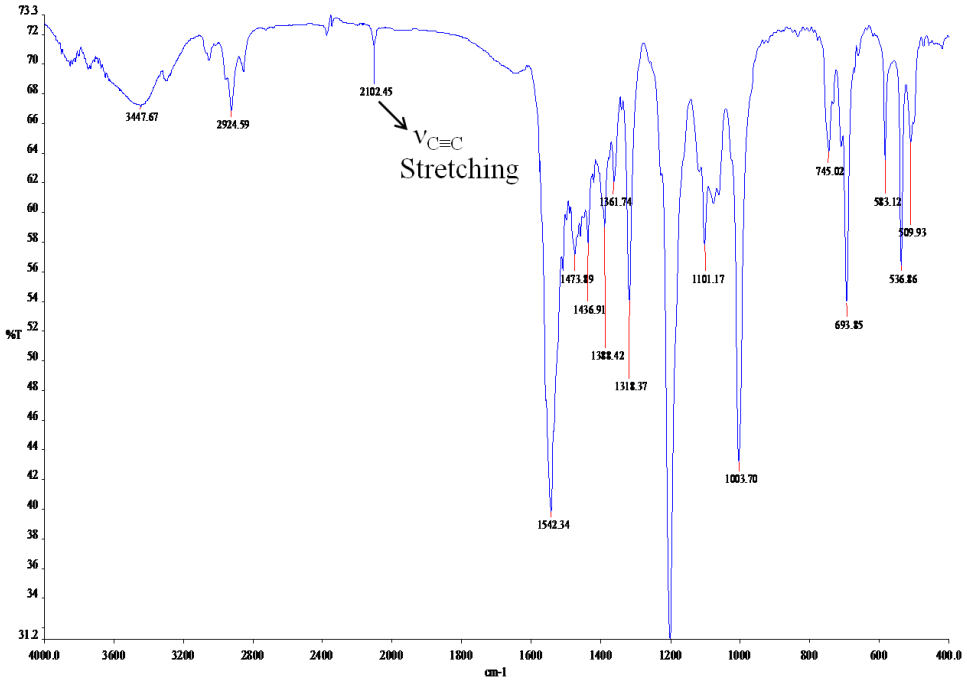

Figure S44. FTIR spectrum of **PBDP2**

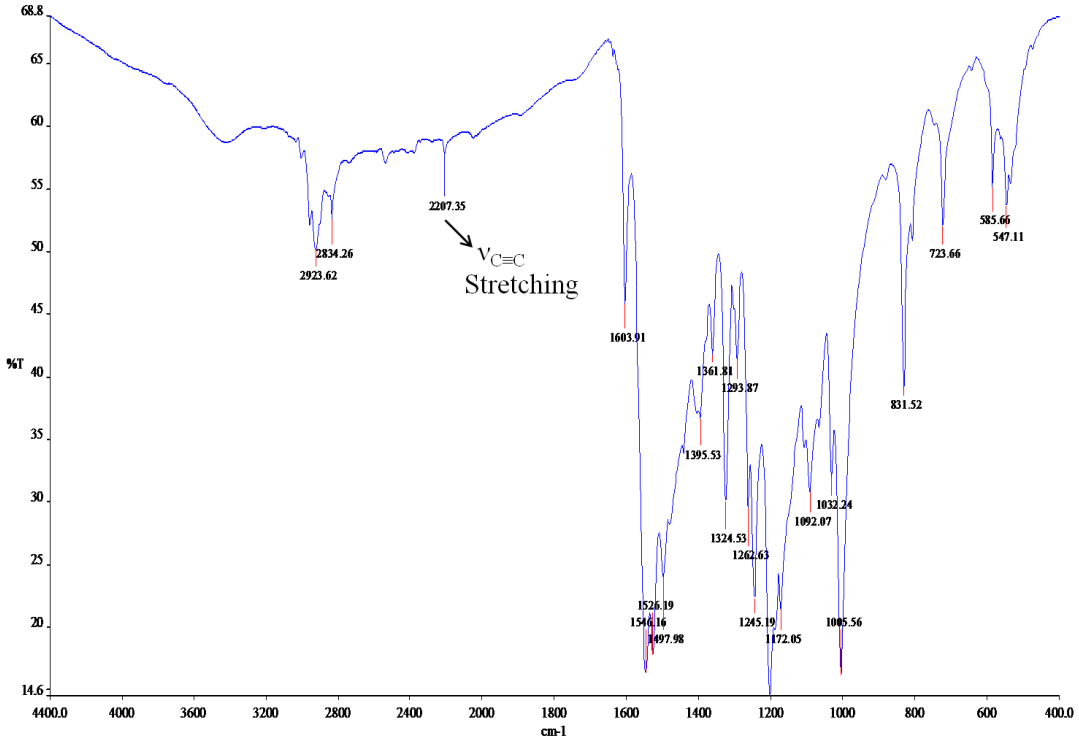

Figure S45. FTIR spectrum of **PBDP3**

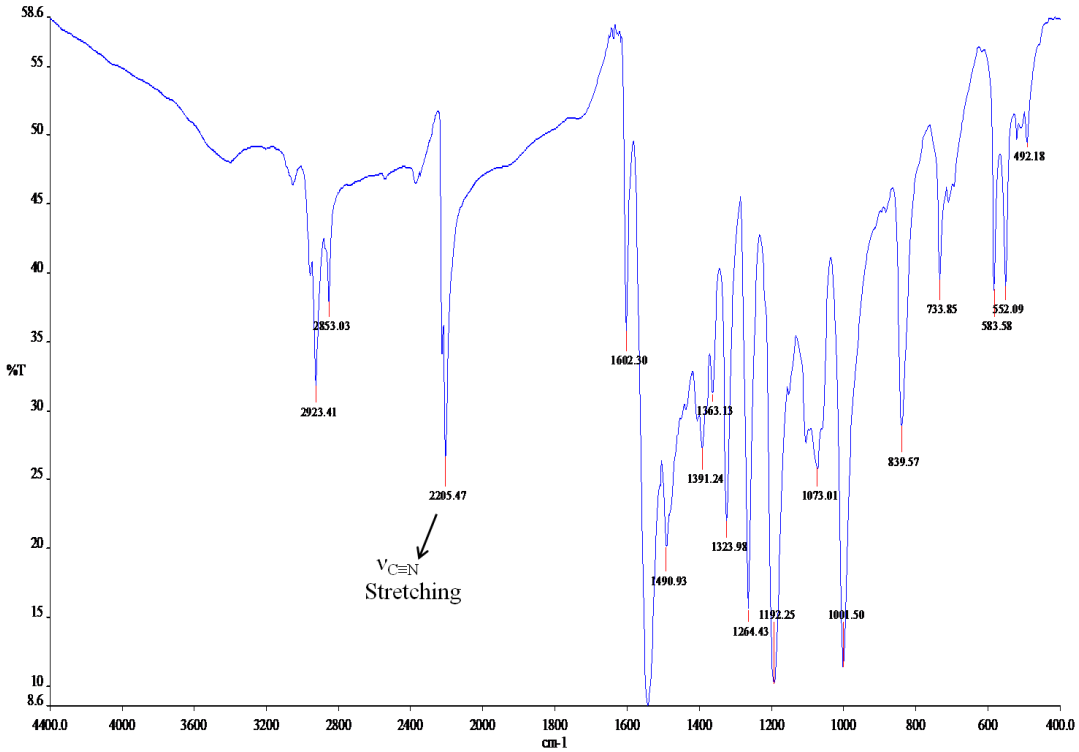

Figure S46. FTIR spectrum of **PBDP4**

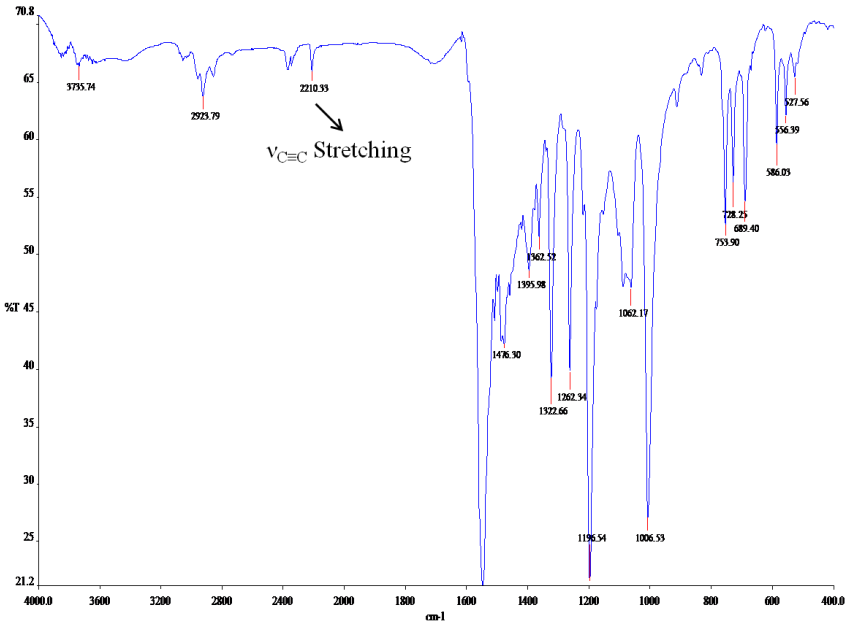

Figure S47. FTIR spectrum of **PBDP5**

1d. HRMS and MALDI-TOF Data

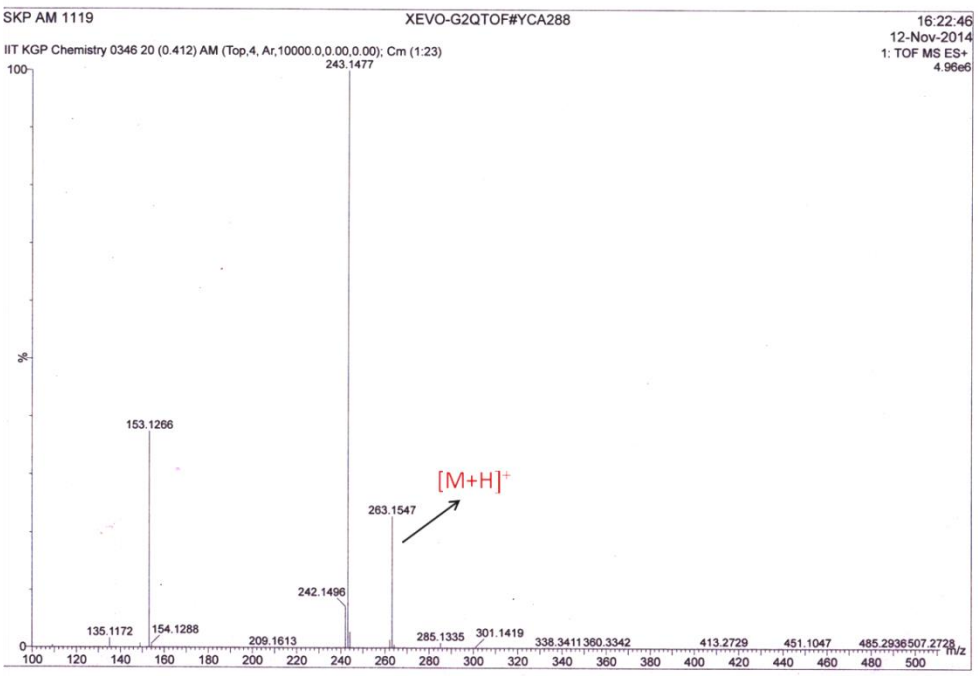

Figure S48. HRMS data of **1**

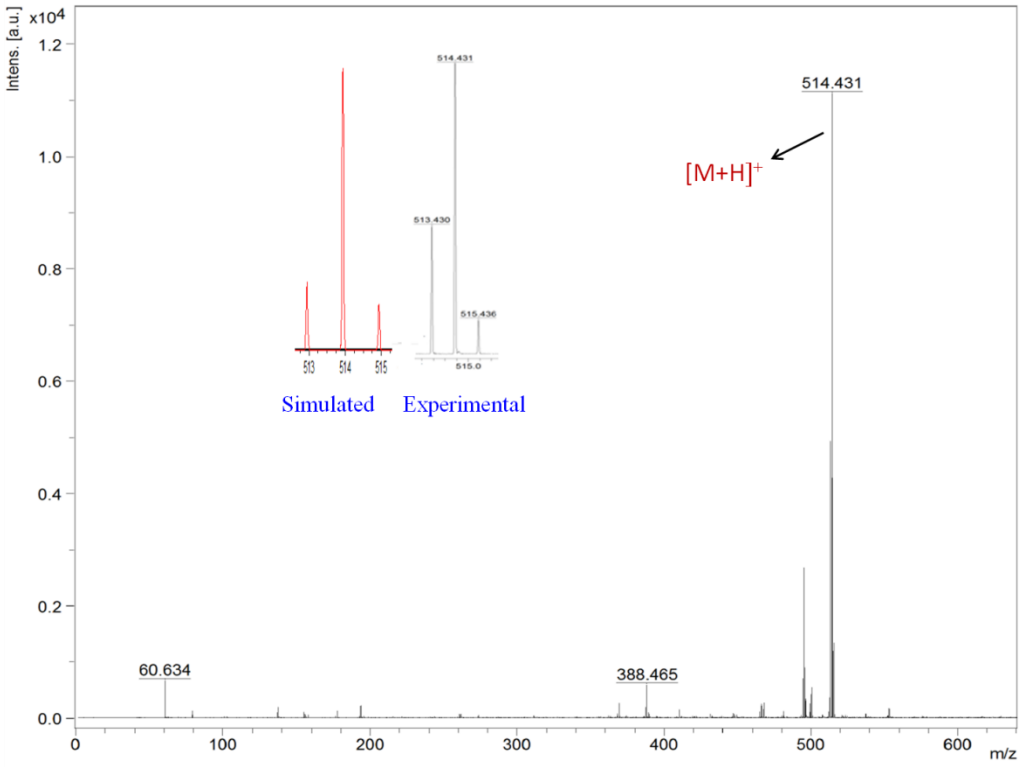

Figure S49. MALDI-TOF mass spectrometry of **2**

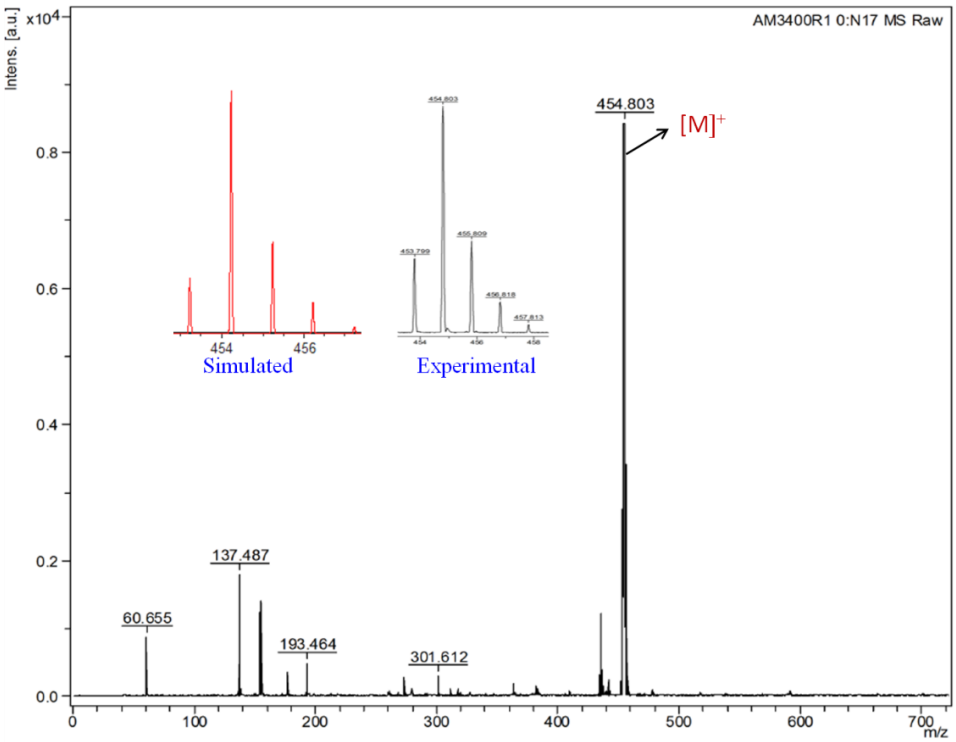

Figure S50. MALDI-TOF mass spectrometry of **3**

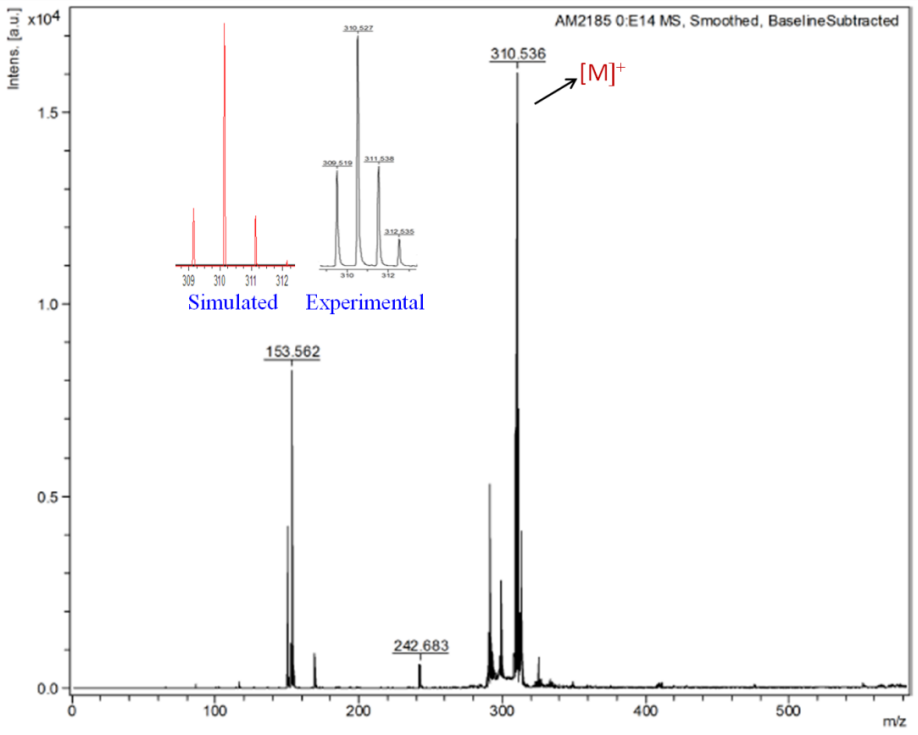

Figure S51. MALDI-TOF mass spectrometry of **PBDP1**

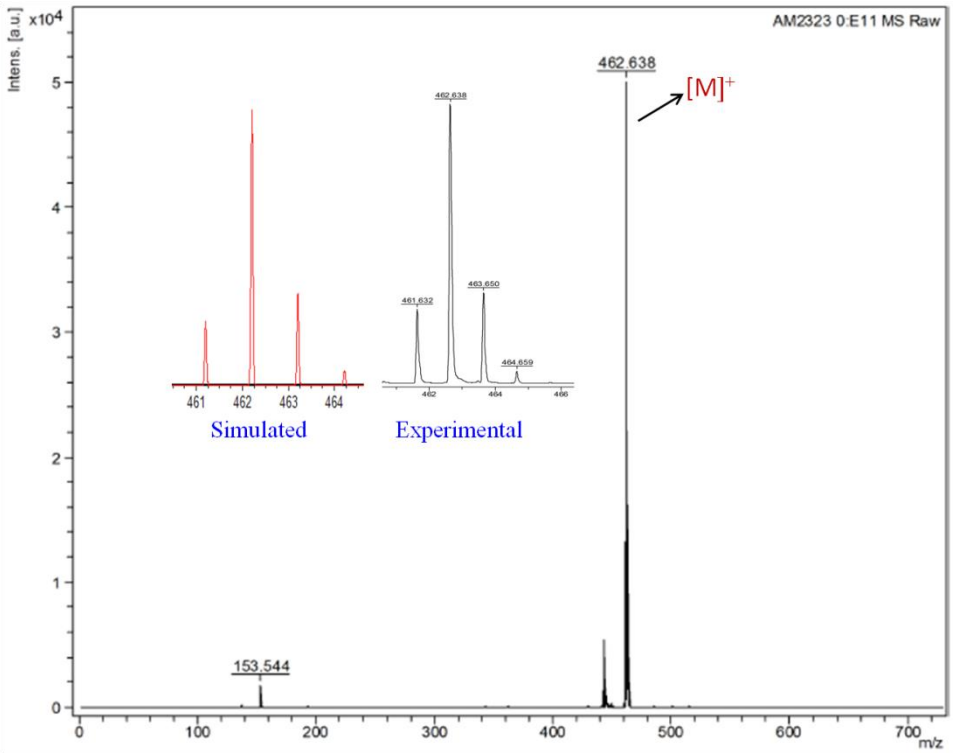

Figure S52. MALDI-TOF mass spectrometry of **PBDP2**

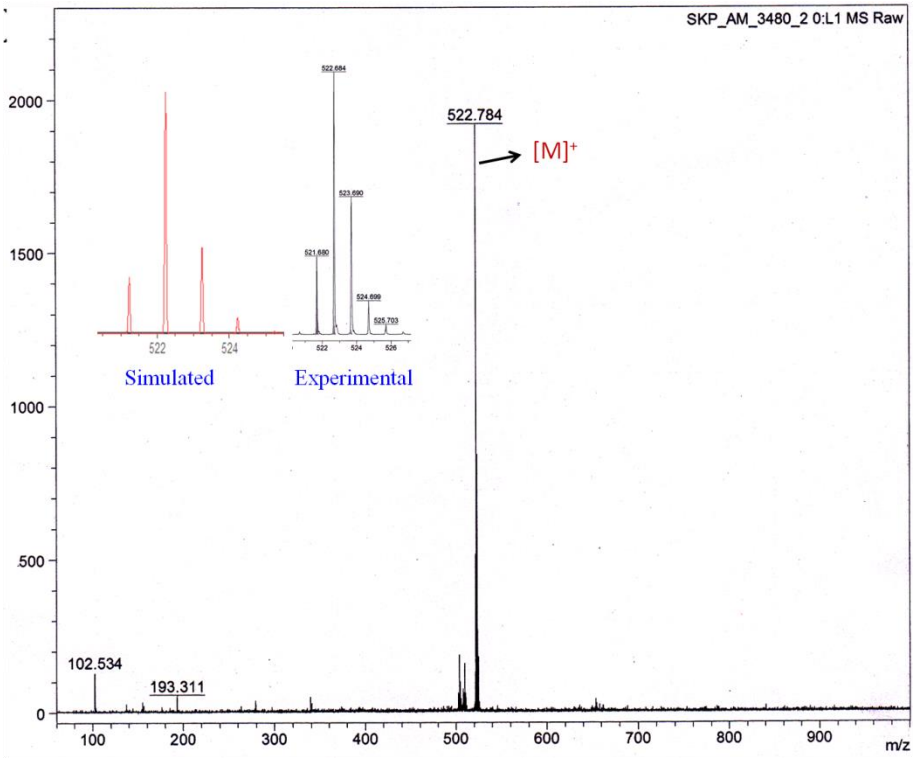

Figure S53. MALDI-TOF mass spectrometry of **PBDP3**

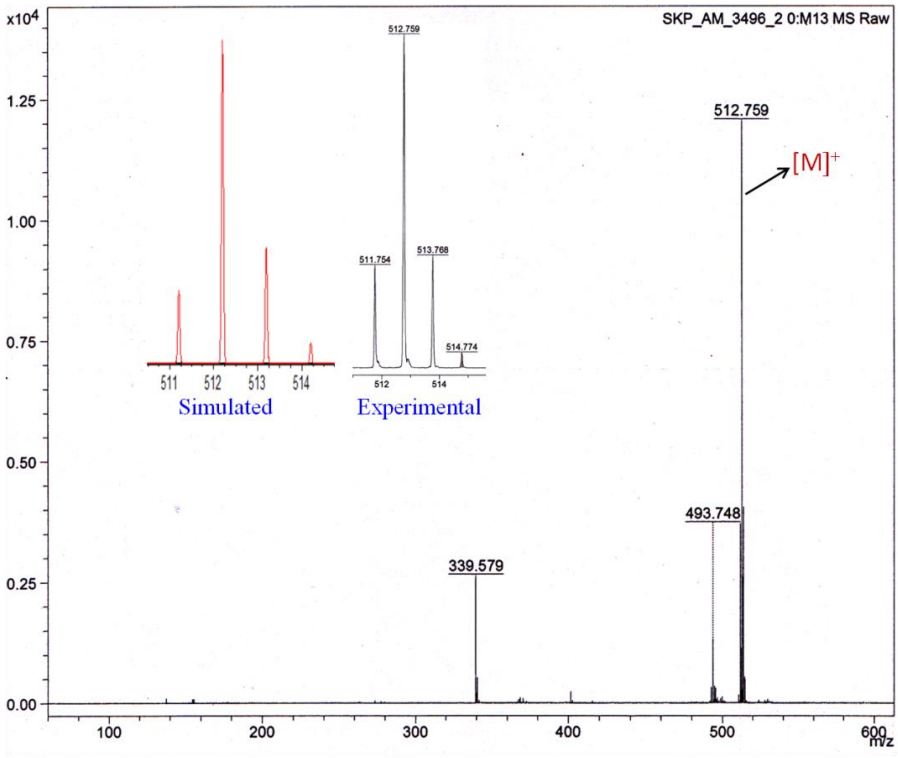

Figure S54. MALDI-TOF mass spectrometry of **PBDP4**

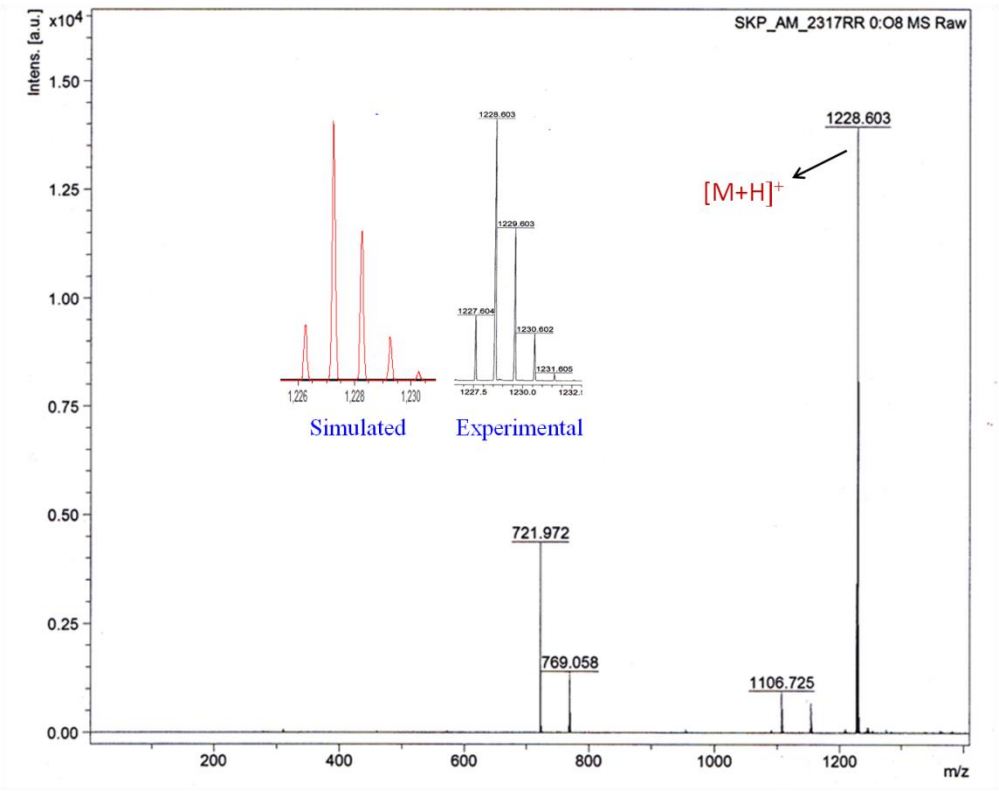

Figure S55. MALDI-TOF mass spectrometry of **PBDP5**

1e. CHN analysis

DATE 09 03 16 TIME 15 19 33 OPERATOR ID CHEMISTRY

RUN 42 ID SKP AM 2317 WEIGHT 1.401

SIGNALS

ZR 5479
NR 6755
CR 16521
HR 18659

CARBON 52.01%
HYDROGEN 4.01%
NITROGEN 2.51%

Figure S56.CHN data of **PBDP5.**

2. Photophysical and lasing studies

2a. Determination of Quantum yield:

All the UV−Vis absorption and fluorescence emission spectra were collected using a Shimadzu UV−Vis spectrophotometer (model UV 2450) and a Spex Fluorolog-3 spectrofluorimeter (model FL3−11) respectively. Throughout all the measurements, the concentration were maintained at (1×10^{-5}) M. Fluorescence quantum yields were measured with respect to a secondary standard fluorescein in 0.1 M NaOH (Φ = 0.79) at 298 K.[6] The phosphorescence quantum yields were calculated by using the absolutely measured quantum yield of 9,10-diphenylanthracene in degassed CH_2Cl_2 at 77 K[7]. In both the cases, the sample and standard concentrations were adjusted to obtain an absorbance of 0.1 or less. The following equation was used to calculate the quantum yields[8]:

$$\frac{\boldsymbol{\Phi_S}}{\boldsymbol{\Phi_R}} = \frac{\boldsymbol{A_S}}{\boldsymbol{A_R}} \times \frac{(\boldsymbol{Abs})_{\boldsymbol{R}}}{(\boldsymbol{Abs})_{\boldsymbol{S}}} \times \frac{\boldsymbol{\eta_S^2}}{\boldsymbol{\eta_R^2}}$$

Here Φ represents the quantum yield, (Abs) represents the absorbance, A represents the area under the fluorescence curve, and η is the refractive index of the medium. The subscript S and R denote the corresponding parameters for the sample and reference respectively.

Preparation of thin film for solid state absorption measurement: The quartz substrates (17 x 15 x 1 mm^3) were cleaned in a fresh piranha solution (7:3 mixture of 98% H_2SO_4 and 30% H_2O_2), washed with Milli-Q water, and followed by ultrasonication in alkaline isopropanol and 0.1 M aqueous HCl at 60^{o}C for 1 h each. After careful washing with Milli-Q water, thin films of the compounds were prepared by spin coating on quartz plate. A solution of **PBDP** dyes in dichloromethane (~10^{-3}M) was dropped on quartz plate and it was spin coated at 5000 rpm for 60 second followed by 8000 rpm for 120 seconds.

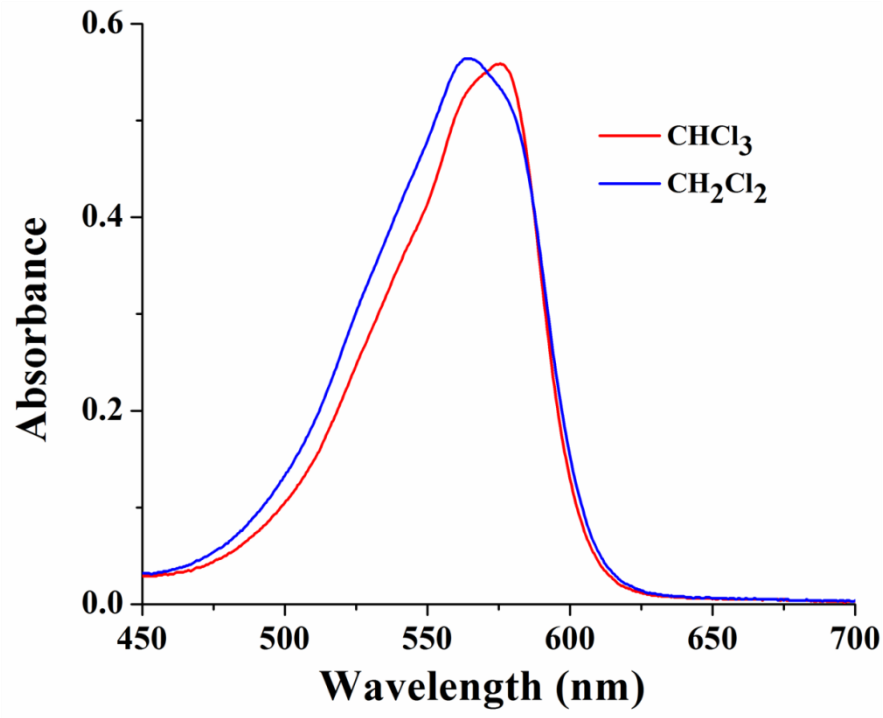

Figure S57. Absorbance spectra of **PBDP5** (1×10^{-5}M) in chlorinated solvents.

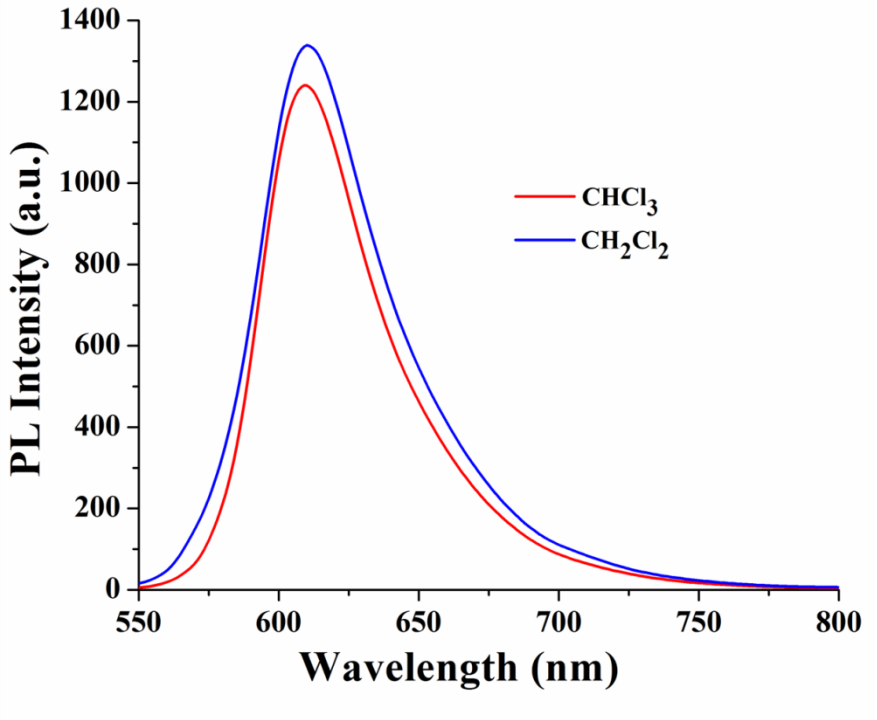

Figure S58. Emission spectra of **PBDP5** (1×10^{-5}M) in chlorinated solvents.

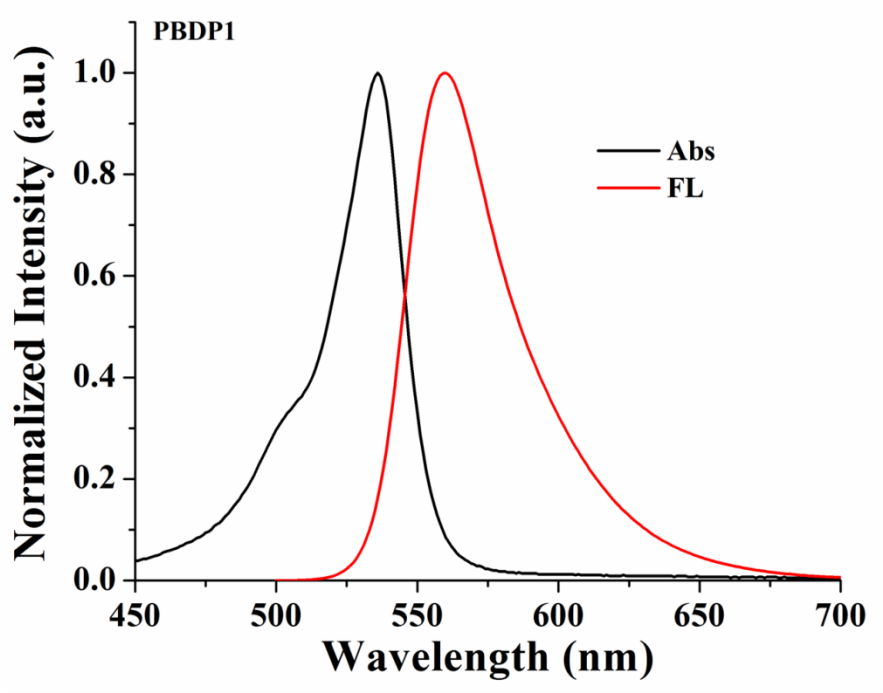

Figure S59. Normalized absorbance (black) and emission spectra (red) of **PBDP1** in toluene.

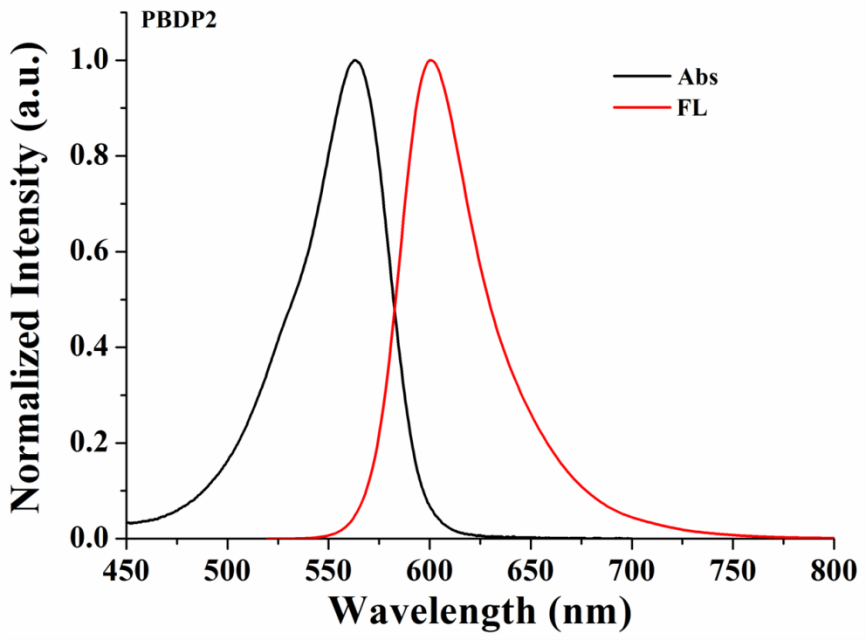

Figure S60. Normalized absorbance (black) and emission spectra (red) of **PBDP2** in toluene.

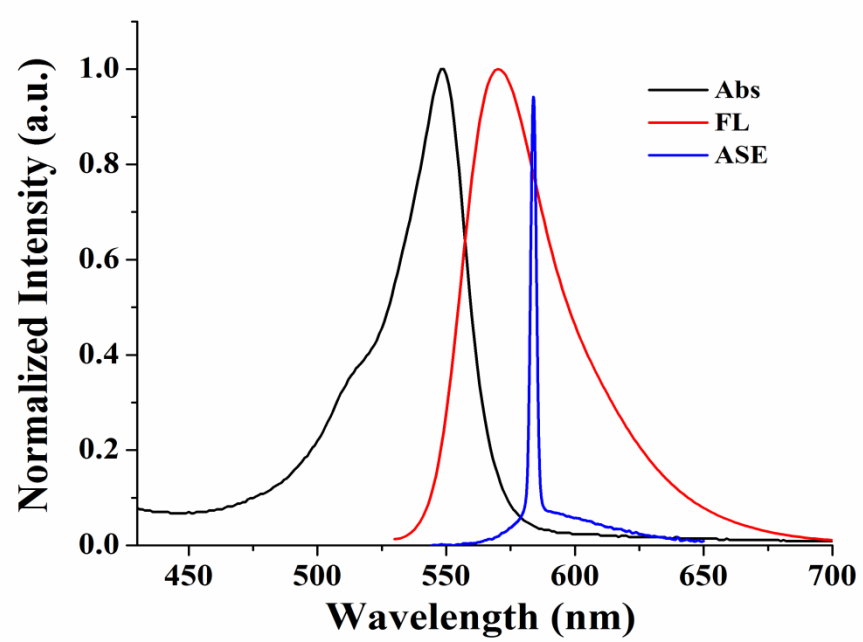

Figure S61. Normalized absorbance (black), emission (red) and ASE spectra (blue) of compound **3** in toluene.

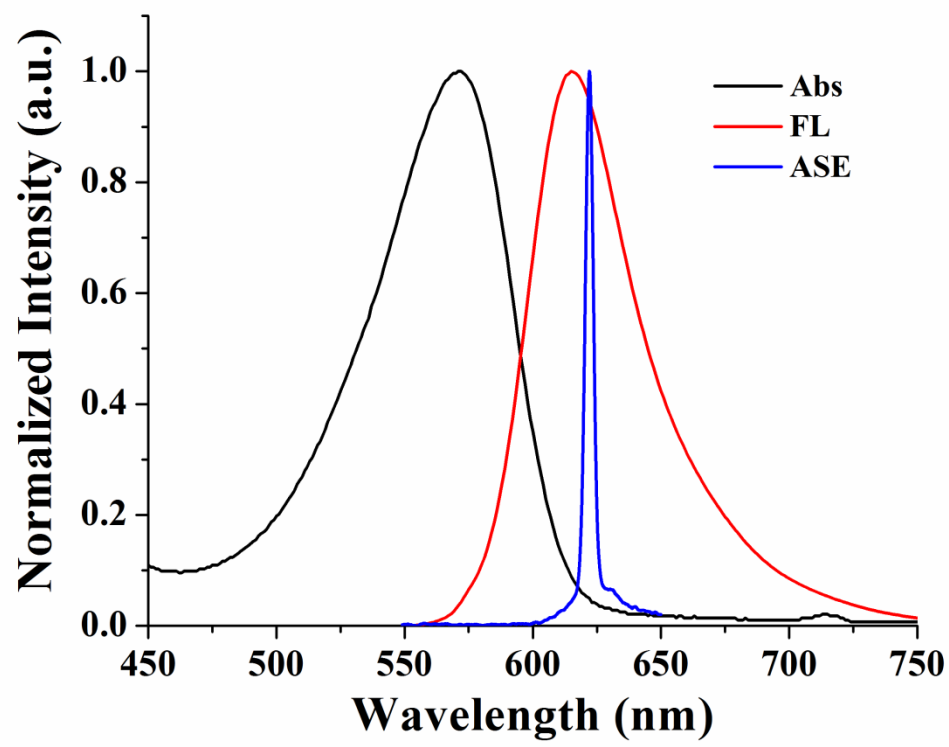

Figure S62. Normalized absorbance (black), emission (red) and ASE spectra (blue) of **PBDP3** in toluene.

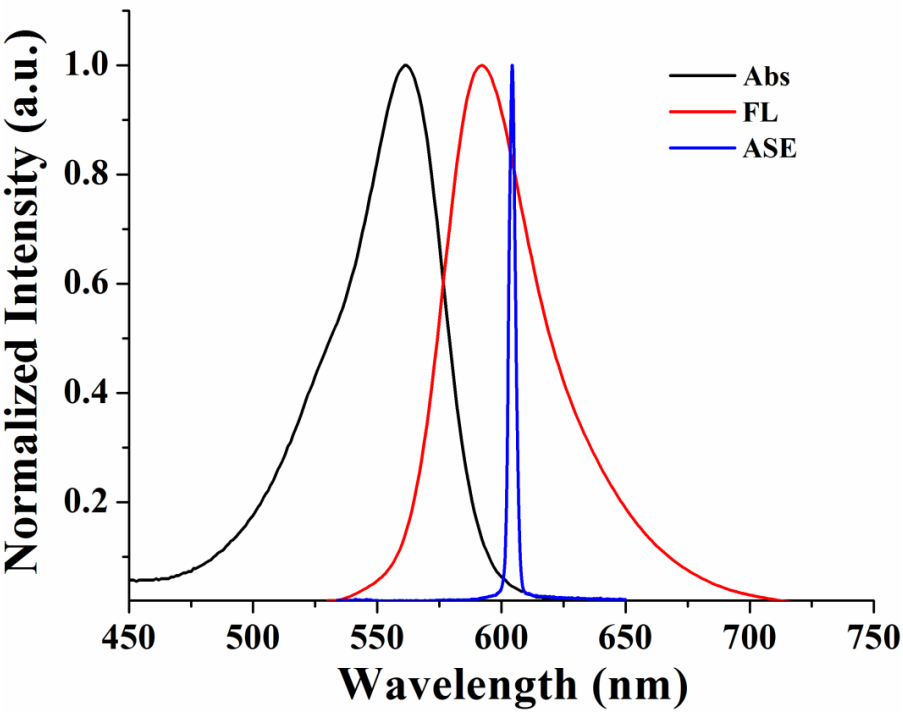

Figure S63. Normalized absorbance spectra (black), fluorescence spectra (red) and ASE spectra (blue) of **PBDP4** in toluene.

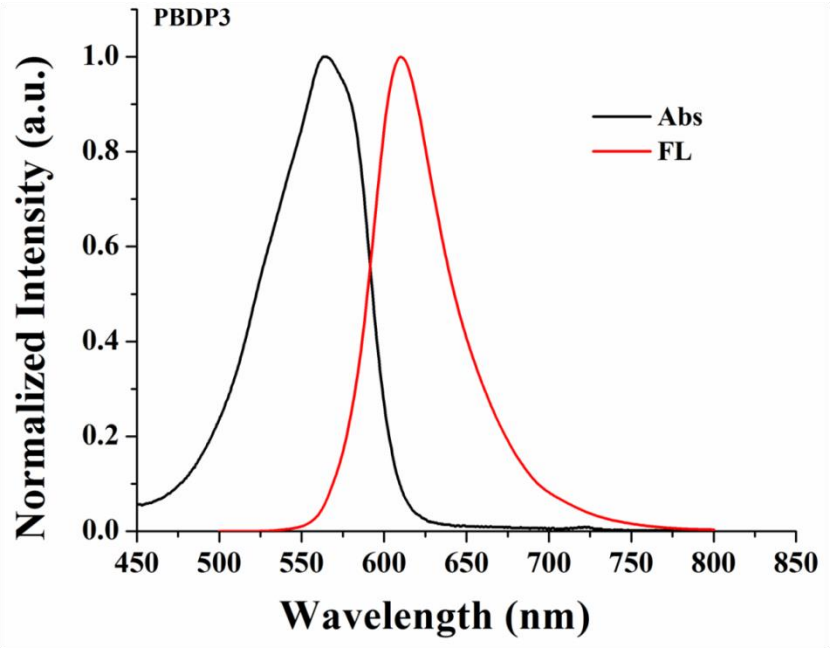

Figure S64. Normalized absorbance spectra (black) and emission spectra (red) of **PBDP5** in CH_2Cl_2 at 300K.

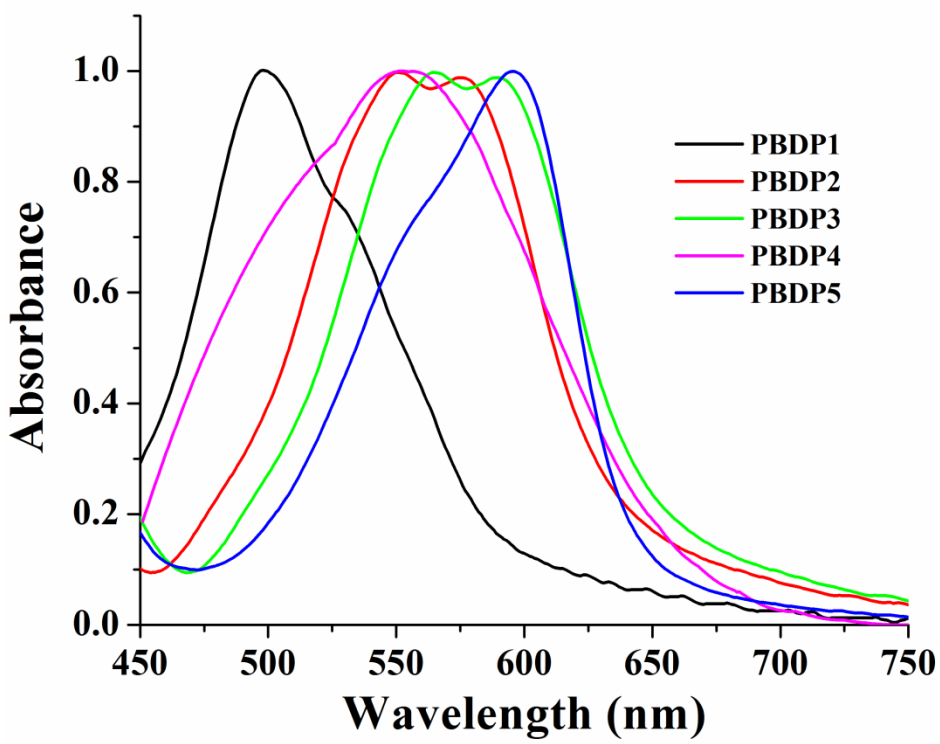

Figure S65. Solid state absorbance spectra of **PBDP1-5**.

Table S1.Absorbance data of PBDP1-5

Compound	Absorption			
	Solution	Thin flim		
	λ_{max}, nm ($\varepsilon\times10^4$ L.mol^{-1}cm^{-1})	λ_{max} (nm)	$\lambda_{max,\ cut\ off}$ (nm)	E_g[a] in eV (Optical)
PBDP1	532(5)	498	642	1.93
PBDP2	561(5.4)	550,576	660	1.88
PBDP3	571(5.1)	565, 589	667	1.86
PBDP4	561(5.3)	554	663	1.87
PBDP5	564(5.6)	595	676	1.83

[a]Calculated using the equation $E_g^{opt}(eV) = 1240/\lambda_{cut\ off}$ [9]

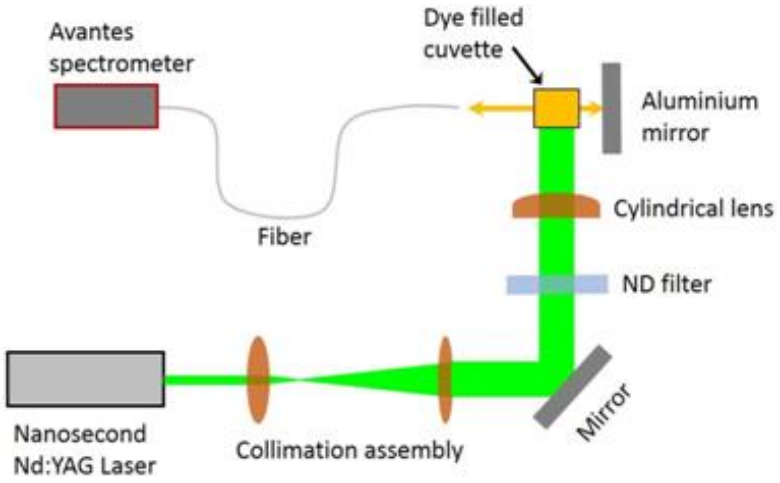

Fig. S66 Experimental set-up used for lasing studies of the synthesized PBDP laser dyes.

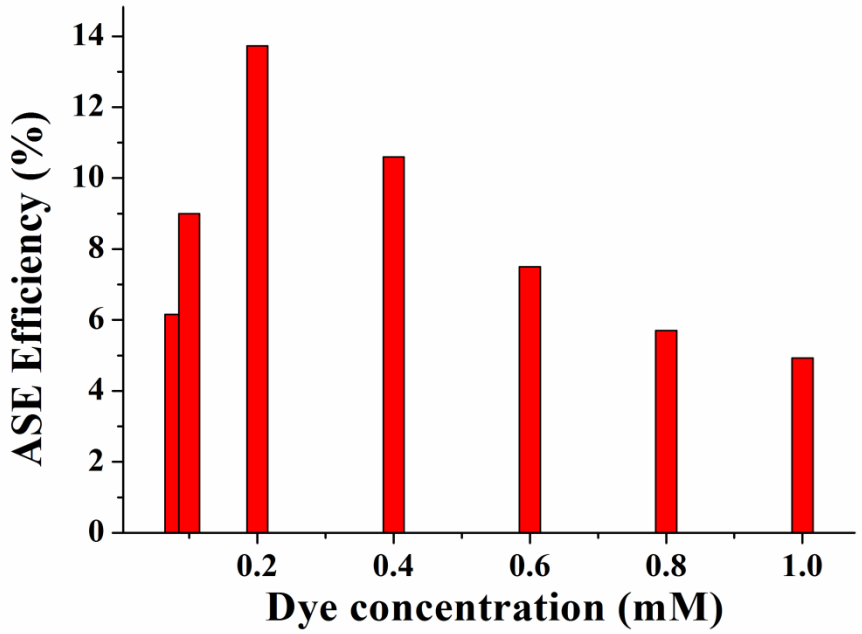

Figure S67.ASE efficiencies of **PBDP3** as a function of dye concentration in toluene solution.

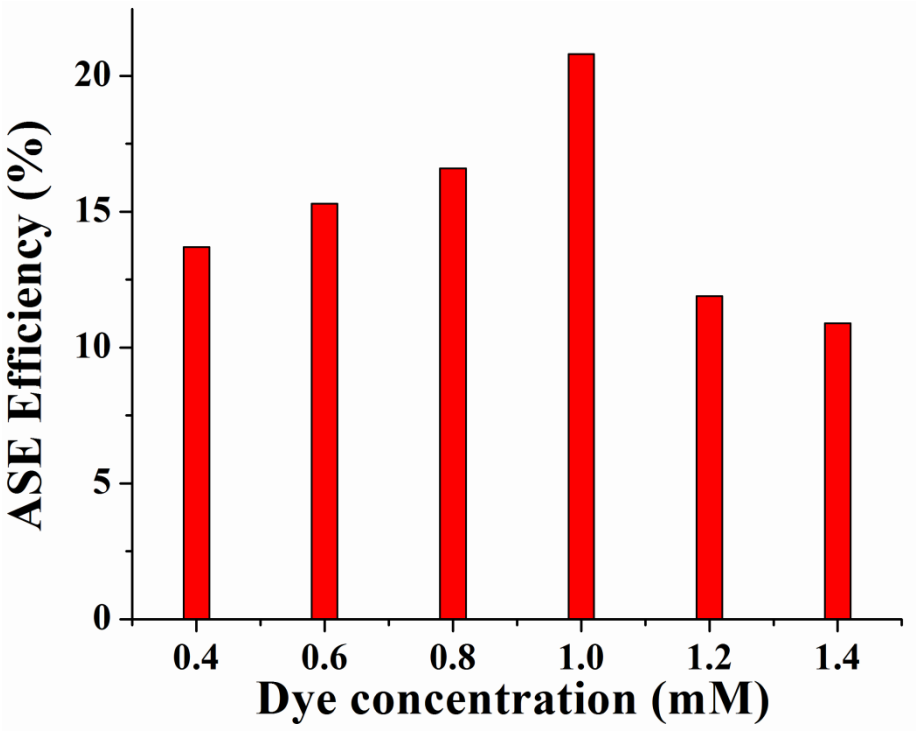

Figure S68.ASE efficiencies of **PBDP4** as a function of dye concentration in toluene solution.

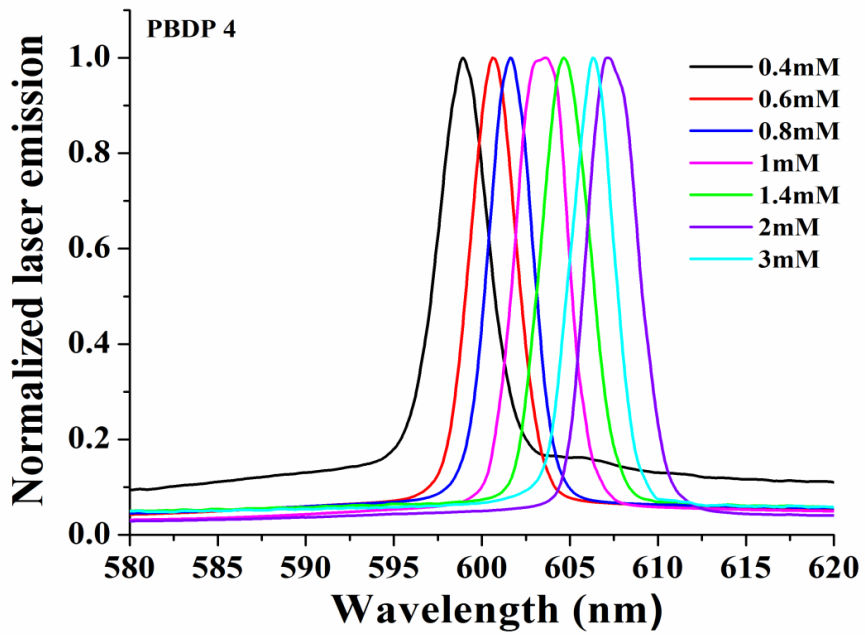

Figure S69. Laser emission spectra of **PBDP4** as a function of dye concentration.

3. Electrochemical characterization

Cyclic voltammetry analysis was carried out in CH_2Cl_2 solution using *n*-Bu_4NPF_6 (0.1 M) as supporting electrolyte, Pt disc working electrode, Pt wire counter electrode and Ag/AgCl reference electrode. The ferrocene/ferrocenium couple occurs at $E_{1/2}$=+0.51 (70) V versus Ag/AgCl under the same experimental conditions. The electrochemical band gap is calculated by using the formula, $E_{g.}= E_{LUMO}- E_{HOMO}$ where E_{HOMO} (eV) = -(E_{Ox} + 4.71) and E_{LUMO} (eV)= -(E_{Red} + 4.71).[10]

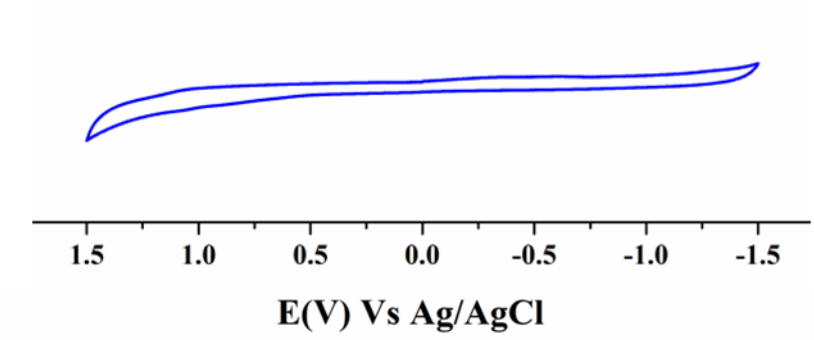

Figure S70. Cyclic voltammogram of DCM using $TBAPF_6$ as supporting electrolyte (Blank run), Pt disc working electrode, Ag/AgCl reference electrode and Pt wire as auxiliary electrode. Scan rate at 100 mV/s.

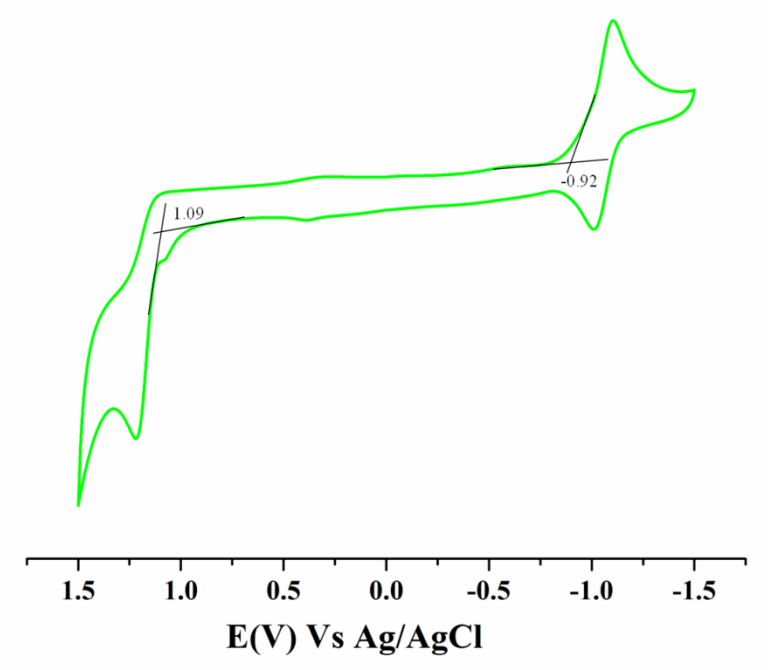

Figure S71. Cyclic Voltammogram of **PBDP1** in DCM showing the onset potential.

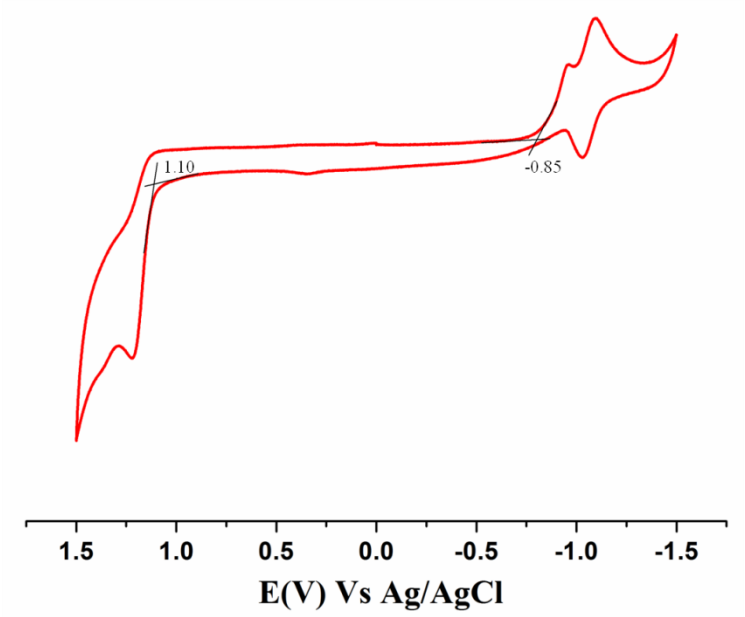

Figure S72. Cyclic Voltammogram of **PBDP2** in DCM showing the onset potential.

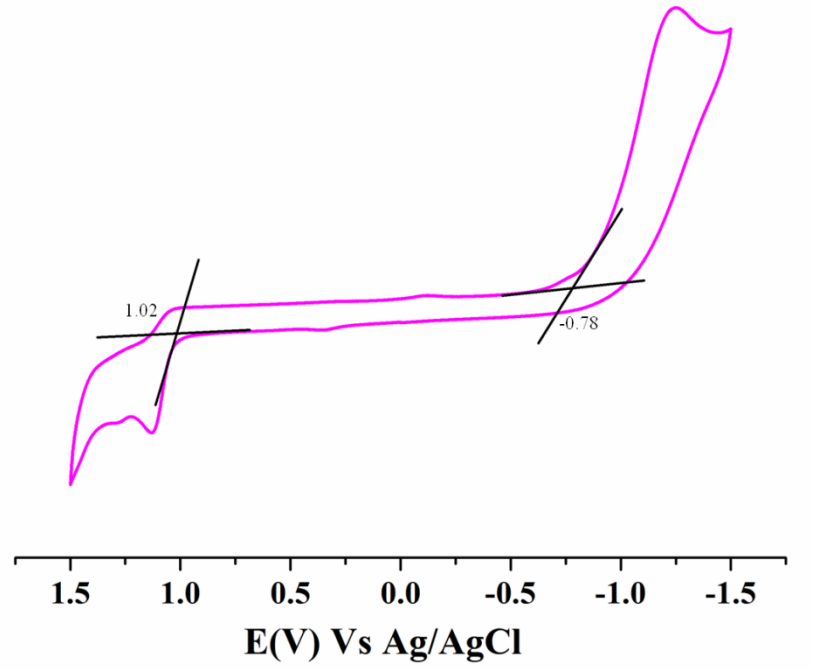

Figure S73. Cyclic Voltammogram of **PBDP3** in DCM showing the onset potential.

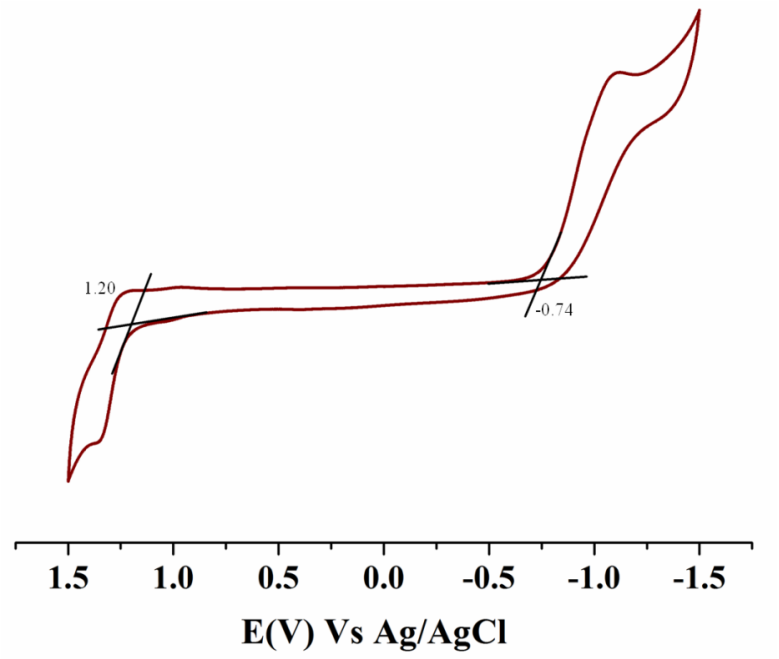

Figure S74. Cyclic Voltammogram of **PBDP4** in DCM showing the onset potential.

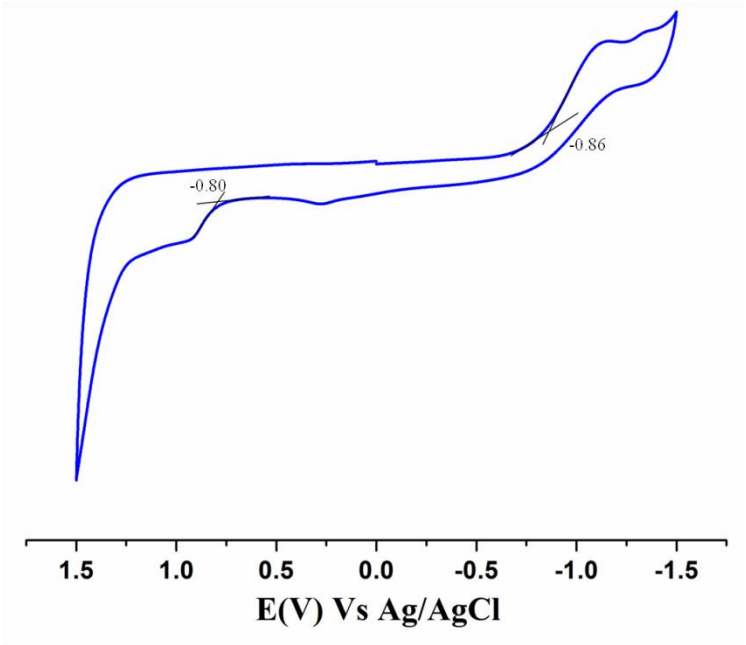

Figure S75. Cyclic Voltammogram of **PBDP5** in DCM showing the onset potential.

4. Crystallographic data

X-ray data collections and refinement: The brownish green colored needle-like single crystals, suitable for X-ray crystallography, were obtained by layering a THF solution of PBDP2 on water. Single-crystal X-ray structural studies were performed on a Bruker-APEX-II CCD X-ray diffractometer equipped with an Oxford Instruments low-temperature attachment. Data were collected at 100(2) K using graphite-monochromated Mo K_α radiation (λ_α = 0.71073 Å). The frames were indexed, integrated, and scaled using the SMART and SAINT software package,[11] and the data were corrected for absorption using the SADABS program.[12] Pertinent crystallographic data for the complex is summarized in Table 5. The title compound crystallizes in the triclinic space group P-1. CCDC 1503390 contains the supplementary crystallographic data for this paper. These data can be obtained free of charge from The Cambridge Crystallographic Data Centre via www.ccdc.cam.ac.uk/data_request/cif. The structure was solved and refined using the SHELX suite of programs.[13] The molecular structure was generated by using ORTEP-3 for Windows Version 2.02.[14] The hydrogen atoms were included in geometrically calculated positions in the final stages of the refinement and were refined

according to the typical riding model. All non-hydrogen atoms were refined with anisotropic thermal parameters.

Table S2 Crystallographic data and refinement parameters for **PBDP2**

	PBDP2
Empirical formula	$C_{30}H_{25}B_1F_2N_2$
Formula weight	462.33
Crystal system	Triclinic
Space group	P-1
a, Å	7.1985(10)
b, Å	11.4552(16)
c, Å	14.805(2)
α, deg	78.169(5)
β, deg	81.599(5)
γ, deg	88.276(4)
V, Å^3	1182.1(3)
Z	2
ρ_{calcd}, g cm^{-3}	1.299
μ, mm^{-1}	0.86
F(000)	484
Reflections	
Collected	15330
independent	4733
observed [I > 2σ(I)]	2455
No. of variables	321
Goodness-of-fit	1.368
Final R indices [I>2σ(I)][a]	R_1 = 0.0593
	wR_2 = 0.1379
R indices (all data)[a]	R_1 = 0.1355
	wR_2 = 0.1773

[a] $R_1 = \Sigma||F_o| - |F_c||/\Sigma|F_o|$ with $F_o^2 > 2\sigma(F_o^2)$. $wR_2 = [\Sigma w(|F_o^2| - |F_c^2|)^2/\Sigma|F_o^2|^2]$

5. References

1. G.Meng, M. L. Zheng and M. Wang, *org. prep. proced. Int.* 2011, **43**, 308.
2. Y. He, M. Lin, Z. Li, X. Liang, G. Li and J. C.Antilla; *Org. Lett.* 2011, **13**, 4490.
3. K. Sugimoto, R. Hayashi, H. Nemoto, N. Toyooka and Y. Matsuya, *Org. Lett*, 2012, **14**, 3510.
4. Y. Lin and Q. Song, *Eur. J. Org. Chem.* 2016, 3056.
5. M. Valàšek, K. Edelmann, L. Gerhard, O. Fuhr, M. Lukas and M. Mayor, J. Org. Chem. 2014, 79, 7342.
6. J. Q. Umberger and V. K. Lamer, *J. Am. Chem. Soc.* 1945, **67**, 1099.
7. S. M. Aly, C. L. Ho, W. Y. Wong, D. Fortin and P. D. Harvey, *Macromolecules*, 2009, **42**, 6902.
8. A. Chakraborty, D. Chakrabarty, P. Hazra, D. Seth and N. Sarkar, *Chem.Phys. Lett.* 2003, **382**, 508.
9. P. Dutta, W. Yang, S. H. Eom, W. H. Lee, I. N. Kang and S. H. Lee, *Chem. Commun.* 2012, **48**, 573.
10. J. Hou, Z. Tan, Y. Yan, Y. He, C. Yang and Y. Li, *J. Am. Chem. Soc.* 2006, **128**, 4911.
11. *SAINT+ Software for CCD Diffractometers*, Bruker AXS, Madison, WI, 2000.
12. G. M. Sheldrick, *SADABS Program for Correction of Area Detector Data*, University of Göttingen, Göttingen, Germany, 1999.
13. (a) *SHELXTL Package, version 6.10,* Bruker AXS, Madison, WI, 2000; (b) G. M. Sheldrick, *SHELXS-86 and SHELXL-97,* University of Göttingen, Göttingen, Germany, 1997.
14. L. J. Farrugia, ORTEP-3 for windows - A version of ORTEP-III with a graphical user interface (GUI) *J. Appl. Crystallography* 1997, **30**, 565.